NON-COVALENT INTERACTIONS IN ORGANIC SYNTHESIS

by

Liangyu Guan

A dissertation submitted to Johns Hopkins University in conformity with the requirements for the degree of Doctor of Philosophy

Baltimore, Maryland

April, 2018

Abstract

By compare to covalent interactions, the strength of non-covalent interactions is relative weak. While it also provides flexibilities to non-covalent interactions. During past decades, the nature of different kinds of non-covalent interactions had been gradually revealed through both computational and experimental methods. Non-covalent interactions had been applied into molecular self-assembly and supramolecular chemistry, but the roles and applications of non-covalent interactions in organic synthesis are still not been well developed. This research focus on the roles and applications of non-covalent interactions in organic synthesis. We demonstrate that a Diels-Alder reaction of a borole can be accelerated greatly by the presence of an appropriately configured C-F bond in the dienophile. Calculations show that the interaction between B and F is the prime instigator in the reaction chemistry, and that the magnitude of this non-covalent interaction is maximized in the transition state. Non-covalent interaction can also affect electrophilic aromatic substitution (EAS). One of the "iron laws" of EAS is that an electron-rich arene will react more rapidly than an electron-poor ring with suitable electrophiles. In this research we present unique examples of electron-deficient arenes instead undergoing preferential substitution in intramolecular competition with more electron-rich rings. These results were made possible by exploiting the heretofore unknown propensity of a hydrogen-bonding OH—arene interaction to switch to the alternative HO—arene interaction in order to provide activation. In an extreme case, this through-space HO—

arene activation is demonstrated to overcome the deactivating effect of a trifluoromethyl substituent, making an otherwise highly electron-deficient ring the site of exclusive reactivity in competition experiments. Additionally, the HO—arene activation promotes tetrabromination of an increasingly more electron-deficient arene before the unactivated "control" ring undergoes monobromination. Non-covalent interactions in this research showed their effects on organic synthesis. It may provide a reference to other related researches, as well as new strategies in organic synthesis.

Advisor: Professor Thomas Lectka

Reader: Professor J.D. Tovar

Reader: Professor Lan Cheng

Acknowledgements

When I stepped into Johns Hopkins University in 2014, I was 25-years old and didn't know too much about organic synthesis. First year courses to me is a challenge, but instructors of those courses are really helpful. I am so thankful for the support of my advisor Prof. Thomas Lectka, who showed me the road to science and allowed me throw all my time into courses in first year to strengthen my background knowledge. This thesis would not be finished without his patience, carefulness and immense knowledge. His guidance helped me in my research and study all the time during last four years.

Besides my advisor, I would like to thank Prof. Tovar and Prof. Klausen. Their instruction on physical organic chemistry and organic synthesis formed foundation of my knowledge in this field. And Their suggestion on my research proposal are really helpful. I would like to thank Prof. Cheng, he gives me a lot help on theoretical and computational chemistry. Their encouragement and help are solid support of this thesis. I would like to thank Prof. Yirong Mo in WMU, with his help I had the chance to study in US and got my Master's Degree. Also, I would like to thank the Chemistry Department of Johns Hopkins for giving me this precious opportunity of studying chemistry.

Life is not only the research. During last four years, support from my family and friends also are my driving forces. Thank my parents and my grandparents, they give me life and rise me up. Thank my fiancé, support from her in past 6 years made her also a part of this thesis. Thank all my labmates and friends, I can have a lot happy times during this period.

Table of Contents

List of Tables

List of Figures

List of schemes

Chapter 1. Introduction

The scale of chemistry research is usually between physics and biology, the size of small and simple molecules are less than the nanoscale, while for large and complex molecules, their size may reach to ~100 nm. The attractive interaction between atoms, ions or molecules were called chemical bonds. Before the 20th century, the description of chemical bonds was mostly based on intuition and empirical studies[1], but there was a breakthrough at the beginning of the 20th century. With the development of quantum theory, the chemical bond can be accurately described by mathematical equations[2] in this period. On the other hand, most of the basic concepts in chemistry were also raised up at this time, such as dipole moment, atomic orbital, isotope, etc. Quantum chemistry also established at this period, along with valence bond theory and molecular orbital theory[2,3].

Because of different behaviors of valence electrons, chemical bonds would have different characteristics. Although there is no clear line between different types of chemical bonds, it is still useful for humans to understand the interaction between atoms by sorting out these interactions into different categories. Covalent interactions and non-covalent interactions belong to two main categories and have different stages. In the research of chemical reactions and molecular properties, the nature and characters of covalent bonds are emphasized. For example, the polarity, electrophilicity or nucleophilicity site, and reactivity of molecules are originated from strong interaction between atoms, which are covalent bond. In other fields, like the research about super-molecules, polymers, liquid-

crystals, enzymes or other biomolecules, the role of non-covalent interactions would be emphasized. The properties of these materials can be affected or modified by many different types of non-covalent interactions, such as hydrogen bonds or halogen bonds.

1.1. Non-covalent interaction:

Covalent bonding involves the sharing of electron pairs between atoms; electrons may come from both atoms or from only one atom. Based on the characters of bonding electrons, covalent bond can be assigned to different groups. Covalent interactions include σ-bonding, π-bonding, metal-to-metal bonding, agostic interactions, bent bonds, and three-center two-electron bonds. Other than covalent interactions, which have been studied in depth over the past few decades. Non-covalent interactions didn't get enough focus until the 1980s, when the Nobel Prize for Chemistry was awarded to Donald J. Cram, Jean-Marie Lehn, and Charles J. Pedersen in recognition of their work in supramolecular chemistry. From then on, researches on non-covalent interactions grabbed lots attentions and developed rapidly. The critical roles of non-covalent interactions in supramolecular chemistry, biochemistry, nanotechnology and even in organic synthesis were recognized gradually. To help people get a better understanding of non-covalent interactions, they were also being assigned into different categories. Based on the characters of non-covalent interactions, they were classified as Van der Waals forces and secondary bond. In the past half century, the roles of the non-covalent interactions in materials technology, catalysis, medicine, and even in data storage and processing have been gradually revealed, with many successful

applications.[4–7]

Among all types of non-covalent interactions, the nature of ionic interactions and hydrogen bonds are clear, both of them driven by electrostatic interactions. Van der Waals Forces also can be classified as electrostatic interactions, because they originated from dipoles, ether permanent dipoles (which generated by polar covalent bonds in asymmetry molecules) or induced dipoles. Based on the different dipole forms, Van der Waals Forces were assigned to three different types, include permanent dipole-dipole interactions (Keesom force), dipole-induced dipole interactions (Debye force) and induced dipole-induced dipole interactions (London dispersion forces). The concept of Van der Waals Forces was fist mentioned in 1873 to represent intermolecular interactions, but the origins of Van der Waals Forces were not completed revealed until 1930s after the foundation of quantum chemistry. The first directly measurement of Van der Waals Forces succeed in 2013, which is more than 100 years after the birth of this concept.

When π-systems were involved in non-covalent interactions, they would be named as π-effects or π-interactions, which includes π-π interactions, cation-π & anion-π interactions, and polar-π interactions. These types of interactions played important roles in biological systems, especially for cation-π interactions, which usually can provide a significant amount of binding enthalpy. π-interactions have important contributions in building protein structures and protein-ligand recognition. Researchers had observed that π-systems are widely existed in proteins. For example, the structure of acetylcholine esterase includes 14 highly conserved aromatic residues, which can form stable cation-π interactions.

The hydrophobic effect is the observation of non-polar molecules aggregation in aqueous solutions. The origin of the hydrophobic effect is not fully understood. It may be caused by the difference in strengths between different non-covalent interactions in solution. There are increasing number of concepts about non-covalent interactions that were raised up in past years. Researches in these fields are providing more information now. It includes the nature of different non-covalent interactions and more applications in other related fields.

1.2. Typical non-covalent bonds

The interactions between two or more moieties usually involve several types of forces. The combination of these interactions can be called the non-covalent bond. Some of typical non-covalent bonds have unique characteristics; thus, a specific name can be used to describe them. The most widely accepted of which includes hydrogen bonds, halogen bonds, chalcogen bonds, pnicogen bonds, etc. Though no electron pairs are shared in non-covalent interactions, electron transfer will still occur. For different kinds of non-covalent bonds, the electron transfer intensity varies.[8] Among these non-covalent bonds, the bond energies are usually around 1-5 kcal/mol[9,10], but in some situations the bond energies can be up to 30 kcal/mol.[11]

The most well-known non-covalent bond is the hydrogen bond, and it has received a lot of attention since it was first defined by Pauling.[12] A clear definition of hydrogen bond established by IUPAC at 2011. “The hydrogen bond is an attractive interaction between a

hydrogen atom from a molecule or a molecular fragment X–H in which X is more electronegative than H, and an atom or a group of atoms in the same or a different molecule, in which there is evidence of bond formation".[13] The hydrogen bond is dominated by electrostatic interactions, while electron transfer still occurs from hydrogen bond acceptor to donor. Though the bond angle of a hydrogen bond prefers to be 180°, the bond strength is not sensitive to the bond angle[11]. During the formation of hydrogen bond, X-H bond vibration frequency may undergo a red-shift or blue-shift. The nature of hydrogen bond red/blue shifts is still under debate, while a widely accepted explanation is that there is no fundamental difference between the blue/red shift of the H-bond. It only caused by the competition between electrostatic repulsion and rehybridization, which can also be expressed as electron transfer.[14–16]

The halogen bond is a similar non-covalent interaction; it can be noted as R–X···Y. Halogen atoms are commonly known as negative charged centers, but through anisotropy in the electron density, a positive charged region called the σ-hole forms at the head of the bond on the halogen atom. Thus, halogen atoms can work as both Lewis acids and Lewis bases. When halogen atoms act as a Lewis acids during an interaction, this specific interaction is called a halogen bond.[17] Halogen bonds were first discovered in the 19th century, in the complexes formed from amines with iodine, bromine or chlorine.[18,19] But halogen bond didn't get too much attention until the late 20th century when Hassel mentioned the important role of halogen atoms in molecular self-assembly phenomena.[20] The strength of the halogen bond is sensitive to the bond angle, and halogen bond formation

is usually coupled with electron transfer from an electron donor to the σ* antibonding orbital of the R-X bond.[11] On the other hand, the strength of the halogen bond can be increased when there is an electron withdrawing group connected to the halogen atom.[21,22] Early studies of halogen bonds was mostly based on crystallographic methods. The unique property of halogen bonds, like their anisotropic character, has also been applied in material science with the recent boom in material chemistry. There is a lot of research focused on halogen bonding in molecular self-assembly and recognition.[23–25] Also, there are many studies of halogen bonds based on computational methods. The nature of the halogen bond and σ-hole is still under discussion, but electron transfer was accepted as one of the factors in their formation. When halogen atoms work as Lewis acids, the Lewis base can be an amine, water or other halogen atom. Additionally, electrons can come from not only lone pairs but also π bonds. That is the reason why alkenes and conjugated π systems can work as electron donors.[10,23,26] Chalcogen atoms (O, S etc.) and pnicogen atoms (N, P etc.) have similar properties. The σ-hole region also exists around these atoms, thus they can work as Lewis acids. These non-covalent interactions are called chalcogen bonds and pnicogen bonds. The nature of chalcogen bonds and pnicogen bonds is similar to halogen bonds, though there are some difference between them.[9,26–28]

1.3. Energy decomposition analysis

One of the powerful tools to study the non-covalent bond is energy decomposition analysis. Because non-covalent bonds are composed of different non-covalent interactions,

energy decomposition analysis can show details of different non-covalent interactions in one non-covalent bond. There a many different ways to achieve this goal, such as symmetry-adapted perturbation theory or morokuma's energy decomposition analysis. Here is a brief energy decomposition analysis scheme based on block-localized wavefunction (BLW) method. The fundamental assumption in BLW method is that all electrons and primitive basis functions can be divided into different subgroups. In each subgroup, orbitals are constrained to be orthogonal, while orbitals in different subgroups are non-orthogonal[80]. According to BLW method, each subgroup corresponds to one monomer of complex, and electrons will be restricted and localized in different monomers. Based on BLW method, studies of electron transfer across molecule will be feasible without significant increase in computation cost.

It is meaningful to separate the total binding energy into different energy terms, and each energy term can be interpreted as a certain physical meaning, which usually represents a certain type of non-covalent interaction. First, a geometric deformation occurs in monomers, which will distort monomers from their optimal structures to deformed structures, which are parts of optimal supermolecule. The changed energy in this stage is defined as deformation energy (ΔE_{def}). Then, monomers are brought together with no change in their electron distribution, which means only electrostatic energy (ΔE_{elec}) is changed. And then, electron exchange is allowed but electrons and orbitals are still frozen. Here the changed energy is named exchange energy (ΔE_{ex}), as a result of Pauli exchange. In DFT calculations, electrostatic energy (ΔE_{elec}) and exchange energy (ΔE_{ex}) are combined

together as Heitler-London energy (ΔE_{H-L}). By exam each energy terms from the results, we can know whether this non-covalent bond is dominated by electrostatic interaction or by electron transfer.

$$\Delta E_b = \Delta E_{H-L} + \Delta E_{pol} + \Delta E_{def} + \Delta E_{ct} + \Delta E_c$$

1.4. Non-covalent interaction in experimental method and reactivity

Chemical reactions involve bond breaking and formation, the amount of nucleis and electrons will not change during this process; only the state of electrons changed. As we have discussed above, a reaction can be divided into several stages: deformation stage, "Coulomb" stage, polarization stage and electron transfer stage. In the first three stages, every molecular orbital of one fragment will be affected by all other fragments, the energy level for each MO will change—either decreasing or increasing and get well prepared for electron transfer. Finally, in electron transfer stage, electrons will be redistributed among the whole complex, and only relative MO will be affected by electron transfer. On the other hand, because the non-covalent interaction can affect the energy level of the MO, it will finally affect molecular reactivity. In this way, non-covalent interaction can work as catalyst, their flexible interactions formations can help to finish more complex tasks.

Computational chemistry provides researchers with a powerful tool in studies of non-covalent bonds. The nature and properties of non-covalent bonds are predicted by molecular simulations, such as the interact patterns[29,30], the influence on reactions and molecular properties[31], the potential acceptors[32], and their application in other related

fields[7,33,34]. Many of these predictions have been proved by experimental results and experimental chemists step further in this field. In recent several years, halogen bond has been turned out to promote α-C−H amination of ether[35], assistant as Diels-Alder reaction catalyst[36], bromocarbocyclization catalyst[37], and many other organocatalysts roles in many reaction[38–42]

1.5. Summary

There are few challenges in the study of non-covalent interactions. One of them is the weak strength, which indicates non-covalent interaction is not stable and makes it hard to control and observe. with computational methods, the molecule is easy to manipulated to modify the strength of non-covalent bond by ether change interaction distance or adjacent substituents. But in organic chemistry, it is a challenge to achieve this goal. Previously our group had synthesized several rigid molecular structures to study the nature of hydrogen bond and halogen atoms. Based on this structure we successfully observed the fluoronium ion in solution. Non-covalent interactions in this research are also based on this philosophy and showed their effects on organic synthesis. It is our hope that these results may shed light on the research of other non-covalent interactions, as well as new strategies in organic synthesis.

Chapter 2. A C-F Bond Accelerated Diels-Alder Reaction

2.1. Introduction

Recently, fluorine chemistry has become a hot topic, due to the prevalence of fluorinated pharmaceuticals[34] and perfluorinated polymers on the market.[43,44] The addition of fluorine atoms to these substances results in a marked decrease in external reactivity, shown by a resistance to biological metabolism in some fluorinated drugs[45] and the low reactivity of perfluoropolymers like Teflon.[46,47] In some ways these properties have led to a belief that the fluorine atom itself is unreactive and cannot be utilized in reactive chemistry like the other halogens. It is likely that the strength of the C-F bond (~110 kcal/mol) and the tight fashion in which it holds its lone pairs of electrons contribute to this misconception.[48,49] However, this is not always the case C-F bond activations by transition metals,[50–55] silyl cations,[56] and even carbocations[57] are well-established processes; the nucleophilic displacement reactions of benzylic, allylic, and tertiary C-F bonds are also commonplace.[58] On the other hand, reactions in which the C-F bond itself serves as an activating or directing group (anchimeric assistor) are exceedingly rare. For our part, we have recently shown that a C-F bond positioned over the π-cloud of an arene ring can activate it toward electrophilic nitration.[59] In the search for other reactions as candidates for C-F bonds activation chemistry, we focused on other signature processes in organic chemistry, such as the Diels-Alder (D-A) reaction.

The D-A reaction is a signature synthetic process in organic chemistry that allows C-C

bond formation through a [4+2] cycloaddition. The novelty of the reaction comes from the incredibly simple reaction conditions, usually just heat or pressure. However, the reaction can result in several stereoisomers depending on how the dienophile and diene come together (endo/exo), the reactants' symmetry or some combination of both.[60] Due to the prevalence of the D-A reaction in organic chemistry, any method of modifying its reactivity, either to make it faster or more selective, is of great interest to the scientific community. Herein we report on a notably selective D-A reaction between a fluorinated dienophile and a borole. Calculations show that the interaction between B and F is the prime instigator in the reaction chemistry, and that the magnitude of this interaction is maximized at (or very near) the transition state (TS).

2.2. Synthesis

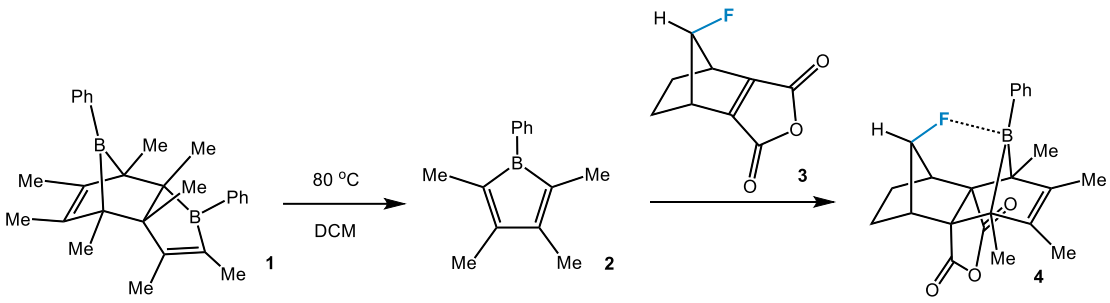

Scheme 1, Diels-Alder reaction of the borole and fluorinated dienophile.

Boroles (boracyclopentadienes) were first synthesized in 1969, but it is only recently that they have been seen as more than a novelty.[61,62] This is likely due to their antiaromatic nature, which results in a high degree of reactivity, especially toward D-A reactions, as well

as extreme air and moisture sensitivity. We synthesized the borole dimer **1** in two steps from dimethylacetylene following the zirconacycle transfer method of Fagan and coworkers.[63,64] When heated at 60 °C, **1** readily converts into monomeric borole **2** (Scheme 1). We imagined that the Lewis acidic boron atom on formally antiaromatic borole **2** could interact in solution with a suitable Lewis base, such as the lone pairs of fluorine in a C-F bond, in an appropriately configured dienophile. Boron's affinity for fluorine has been well documented, and more recently it has seen use in fluoride sensing, often with bidentate boron reagents that can chelate with fluoride ions.[65] Our proposed method reverses the interaction, using the Lewis basicity of fluorine to lure the borole into the reaction. Alkene **3** makes a good candidate, as an interaction between B and F in a hypothetical Diels-Alder TS is stereoelectronically feasible, whereas that between B and the O on the carbonyls is not. The borole dimer and the dienophile were dissolved in DCM and heated at 80 °C to facilitate the retro-D-A reaction of the dimer. We observed that borole **2** reacts rapidly and smoothly to produce a decent yield (45 %) of diastereomerically pure adduct **4**. In our experience, most other Diels-Alder reactions of dienophile **3** afford mixtures of stereoisomers, a fact which suggested that the reaction could be directed by the B---F interaction.[66,67] Another, more interesting question is whether the B---F interaction accelerates the Diels-Alder reaction in this case. It is known that just about all other Diels-Alder reactions of dienophile **3** require forcing conditions, either high temperatures or high pressure.

2.3. X-ray crystallography

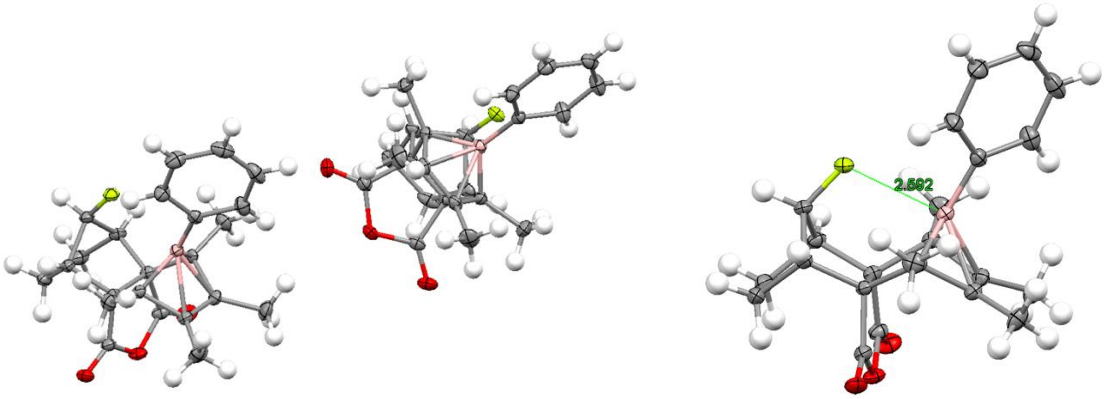

Figure 1. Crystal structure of 4.

A suitable crystal of product **4** was grown from a mixture of DCM and diethyl ether for X-ray diffraction analysis. The crystal is twinned, with the two structures having the phenyl ring rotated in a different conformation. In the crystal, the B and the F are decently separated by 2.592-2.609 Å, depending on the conformation. On the other hand, a strong interaction between B and the vicinal C=C bond is noted. The boron is roughly 1.896-1.936 Å away from the double bond, depending on which rotamer is observed. While the crystal seems to indicate a bonding interaction between the boron and the double bond, the carbon atoms still appear to be sp^2 hybridized. In fact, the methyl groups seem to be tilted slightly upward toward the boron. This interaction is isoelectronic to the 7-phenylnorbornenyl cation, and has been observed in a few other cases.[63,64,68]

We next attempted to hydrogenate the double bond vicinal to the boron, in the hopes that if the boron were free from that interaction, a stronger interaction with fluorine would be observed. However, the bond was unable to be reduced, even under strong hydrogenation conditions (H_2, Pd/C at 50 psi). The bond was also found to be unreactive

to various substitution reactions, such as halogenation and hydration. This is likely a combination of the bond's interaction with boron as well as steric hindrance from the methyl groups on the bond.

2.4. Calculations

DFT calculations (6-311+G**/ωB97XD)[69] on four possible TS's for the reaction are shown in Table 1. Two points worth noting: the free energy of the lowest transition state **5** is negative relative to the starting molecules, a result that points to the existence of a stable precomplex; calculation of this precomplex shows considerable interaction between B and F. As expected, TS **5** is almost 4.3 kcal lower than the closest competitor, largely due to the observed interaction between B and F. Only TS's **7** and **8** are predicted to be less stable than the starting molecules.

Table 1. Relative energy and activation energy of each TS pathway.

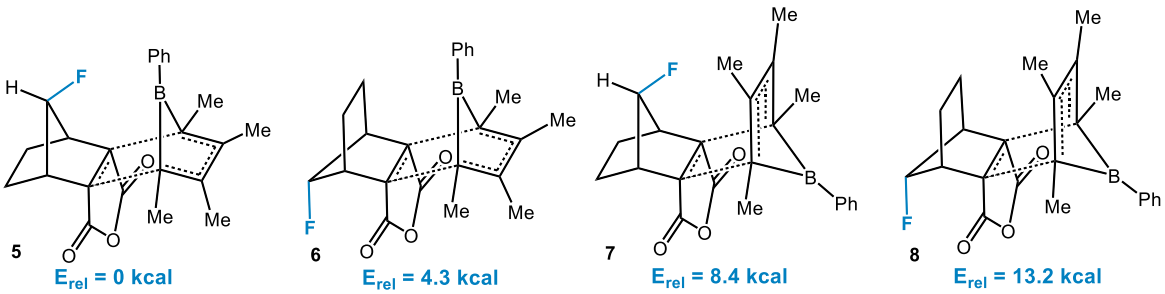

Transition State	E_{rel} (precomplex) (kcal)	E_{rel} (TS) (kcal)	E_{rel} (product) (kcal)	$E_{activation}$ (kcal)
5	0.00	0.00	0.00	6.95
6	-2.18	4.34	-3.40	13.47
7	1.24	8.42	7.57	14.14
8	0.94	13.27	4.66	19.28

Calculations also predict that the reaction proceeds in TS **5** through an unusual trajectory. As the substrates approach one another in the precomplex, the interaction between F and B strengthens, bringing the two atoms closer together (Figure 2a). Once the transition state is reached, the F---B distance is predicted to lengthen again, to be replaced by a strong, through-space interaction with the newly formed vicinal C=C double bond in the product. The F---B interaction seems to act as a "yo-yo" or "piston" in its activating role. In the Diels-Alder adduct, the boron is unusually coordinated - weakly to the C-F bond, strongly in a through-space manner to the C=C bond, and covalently to three carbon atoms to attain a polyvalency. An atoms-in-molecules analysis of the product also shows a bond critical point between B and F, which is indicative of a through-space interaction.[70]

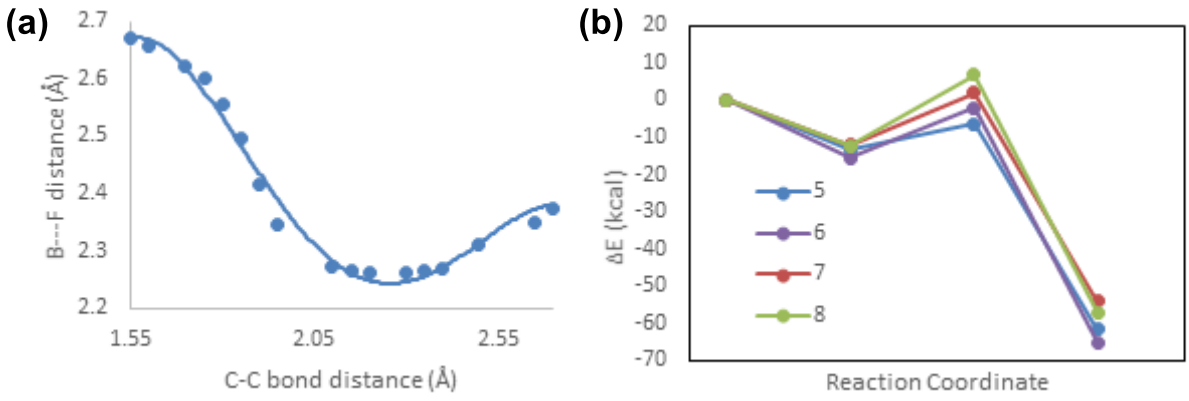

Figure 2. (a) B---F distance during the C-C bond formation in TS 5. (b) Plotted reaction coordinate for the four TS pathways.

2.5. Control experiment

With all the evidence pointing to the B---F interaction providing a strong directing effect, we developed a control experiment to quantify the kinetic consequences of the B---F interaction. In a minimal amount of DCM (3 mL) a fifth of an equivalent of borole dimer **1** was heated at 80 ºC (affording 0.4 equiv. of **2**) with 1 equiv. of the regular dienophile **3** and a second equiv. of a new dienophile **9** in a sealed tube. Dienophile **9** has its fluorine pointed away from the double bond, so any of the DA product would have to form from the comparatively weaker B---H coordination or the borole's own reactivity. Upon workup the observed product was exclusively compound **4**. This indicates the B---F interaction has an impressive effect on the selectivity of the reaction. This directing effect could also be the cause of dienophile **9**'s poor reactivity. If coordination to the fluorine is so favorable, any borole that encounters **9** will coordinate to the fluorine, effectively trapping it on the opposite side of the molecule, unable to react with the double bond.

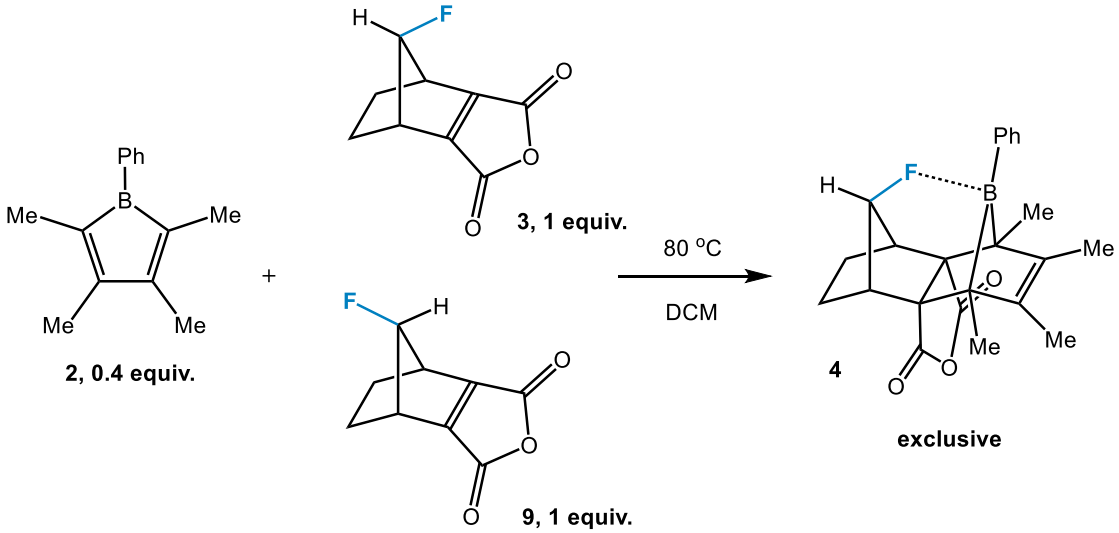

Scheme 2. In- versus out-fluorine competition reaction.

This result is in line with the calculations – the computed free energy of activation leading to the observed product is some 5.2 kcal lower than that leading to compound **10**, the most favorable DA product of dienophile **9**. Although there may be a favorable B---H interaction present in the TS of **10**, the corresponding B---F interaction lowers the energy of its transition state a significant amount.

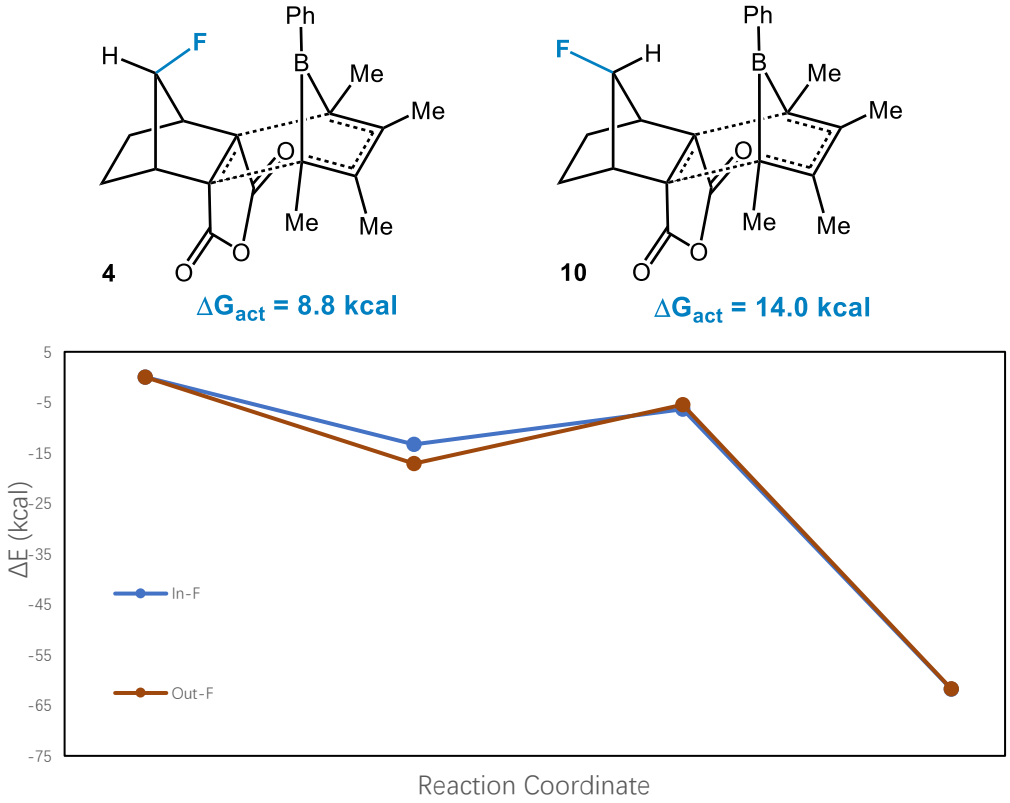

Figure 3. Comparison between the transition state free energies of the Diels-Alder reaction of the in/out-fluorinated dienophiles.

2.6. Conclusions.

We have observed a very selective DA reaction between a fluorinated dienophile and a borole. Interestingly, the source of the selectivity appears to be from a rare case of a fluorine acting as a Lewis base and coordinating to the Lewis acidic p-orbital on the boron. In the

precomplex and TS the fluorine seems to act as a lure, coordinating to the borole and angling it over to react with the double bond. After the DA reaction is complete the boron's p-orbital is preferentially drawn to the newly formed vicinal double bond. However, molecular modeling calculations do indicate that there is still a small interaction between the fluorine and the boron.

Chapter 3. Through-space Activation Can Override Substituent Effects in Electrophilic Aromatic Substitution

3.1. Introduction:

Electrophilic aromatic substitution (EAS) is one of the most fundamentally important reactions in the science of chemistry.[71,72] In the classroom setting, students are taught at length about how EAS reactions are governed by "substit uent effects" in terms of relative reaction rates and selectivity.[73] For instance, imagine that a molecule with two different aromatic rings, separated by a linker, is subjected to an EAS reaction. In principle, substitution will occur at the more electron-rich ring invariably, assuming other factors (e.g. steric effects, chelating directing groups, intramolecular electrophiles) are equal. This deactivating effect on EAS reactions by electron withdrawing groups is well established, and it is a fundamental concept in textbook organic chemistry. On the other hand, what if a traditionally deactivated ring were to experience an external source of activation that would compensate for its inherent unreactivity? This situation is reminiscent of Meisenheimer complexes - anionic σ-adducts formed from the interaction of highly electron-deficient arenes with alkoxide nucleophiles.[74–76] Having that in mind, it stands to reason that if an oxygen-based functional group is poised, at very close distance, to an electron-deficient arene ring in space, its lone pair of electrons should stabilize a Meisenheimer-like transition state[77,78] and thus alter its reactivity toward EAS (Figure 4).[79]

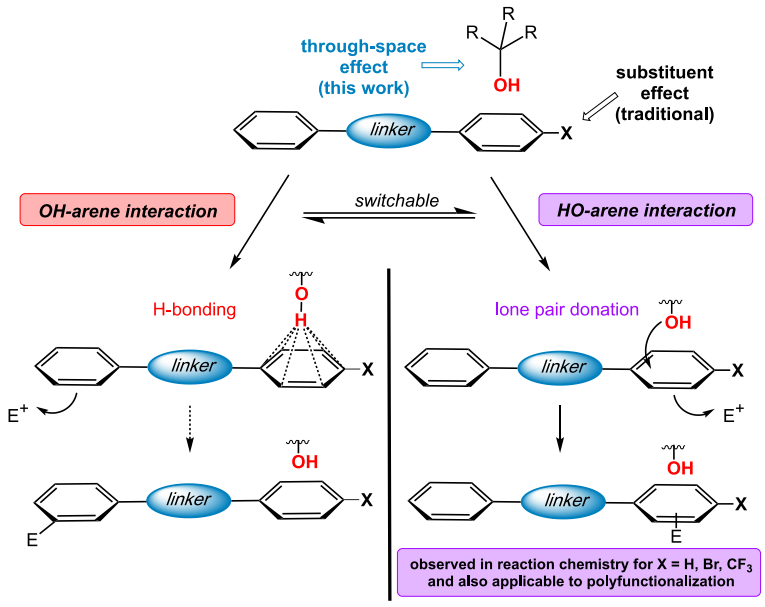

Figure 4. Switchable OH/HO—arene interaction guides non-traditional electrophilic aromatic substitution reactivity/selectivity.

Herein, we present examples of electron-deficient arene rings that undergo preferential substitution in competition with relatively electron-rich rings, whereby through-space interactions override traditional substituent effects. Furthermore, we exploit the heretofore-unknown propensity of a hydrogen-bonding OH—arene interaction to switch to the alternative HO—arene interaction in order to provide the basis for activation. As this complex interaction may influence reactivity, for instance, in enzyme active sites and other supramolecular systems, we have employed a tailor-made "probe molecule" to study this interaction in a rigid, controlled environment. We recently reported an F—arene interaction that achieves through-space EAS activation; we believed the phenomenon would be much stronger with an oxygen atom incorporated in a similar molecular scaffold, thus allowing traditional reactivity patterns to be reversed.[59]

3.2. Synthesis:

To test our initial hypothesis, we chose target molecule **11**, which contains a hydroxyl group poised directly over an aromatic ring (Scheme 3); we envisioned this could assist with EAS through a Meisenheimer-like interaction. The synthesis of **11** is shown in Scheme 3. First, benzylation of previously reported alcohol **12**,[59] followed by saponification and anhydride ring formation, affords alkene **13** (29% yield over three steps). To establish the 'probe' and 'control' rings, a Diels-Alder reaction of anthracene with **13** (160 °C, sealed tube), followed by debenzylation (H_2, Pd/C), provides alcohol **14** (43% yield over two steps). Finally, epimerization of the hydroxyl group in **14** (PCC oxidation, then $LiAlH_4$ reduction) yields the desired alcohol **11** (64% yield over two steps).

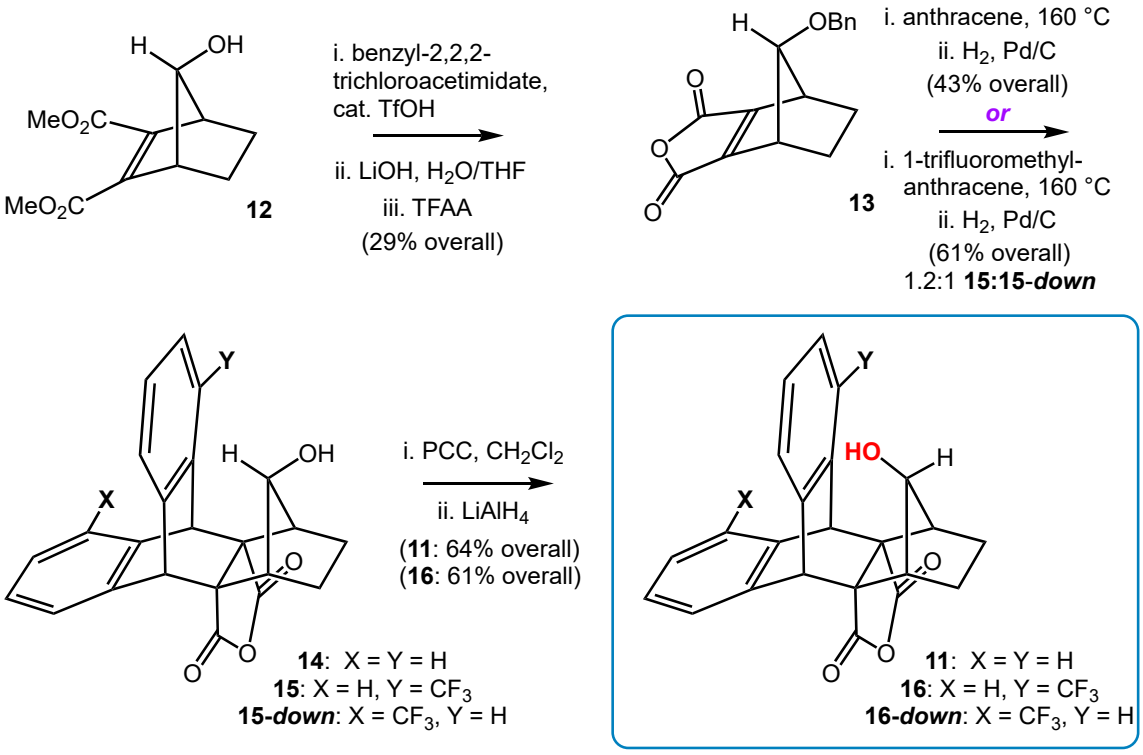

Scheme 3. Synthesis of the probe molecules 11 and 16.

3.3. Physical properties

The OH—arene interaction of **11** is revealed by a red-shifted OH stretch (32 cm^{-1}) in the IR spectrum in chloroform when compared to the *out*-diastereomer **14** (Table 2). In the NMR spectrum ($CDCl_3$), the oxygen-bound proton is strongly shielded (-0.21 ppm) and sharp in comparison to the broader resonance of the OH group in **14**, which is comparatively deshielded (1.16 ppm). Thus, it appears that intramolecular hydrogen bonding to the arene dominates in **11**, similar to interactions observed between OH groups and non-conjugated C=C bonds.[14]

Table 2. Comparison of OH stretching frequencies and OH proton chemical shifts.

Compound	IR -OH (cm^{-1})	^{1}H NMR -OH (ppm)
1 (*in* OH)	3577	-0.21
4 (*out* OH)	3609	1.16
6 (*in* OH CF_3)	3606	0.18
5 (*out* OH CF_3) (mixture)	3609	1.24

* OH stretching frequencies were measured in CH_2Cl_2, OH proton chemical shifts was measured in $CDCl_3$.

The OH—arene hydrogen bond can be categorized, very generally, as a type of cation-π interaction. It has been observed biologically; for example, the OH group of a threonine residue is positioned above the π-cloud of tyrosine in the enzyme glutathione transferase when complexed with glutathione.[80–83] Additionally, a water—phenylalanine interaction is featured in the complex of the anti-Alzheimer's drug donepezil with its target acetylcholinesterase.[84,85] In the case of small molecules, although a number of well-

documented examples exist in the literature,[86–92] many aspects of the interaction remain unexplored. n terms of intermolecular interactions, OH—arene hydrogen bonding plays an important role in the formation of 1,1,2-triphenylethanol dimers in the solid phase.[93] In addition, several short contacts between hydroxyl groups and arenes can be found in a search of the Cambridge Structural Database (CSD), though in those cases the interaction was not the focus of study.[94,95]

3.4. X-ray crystallography

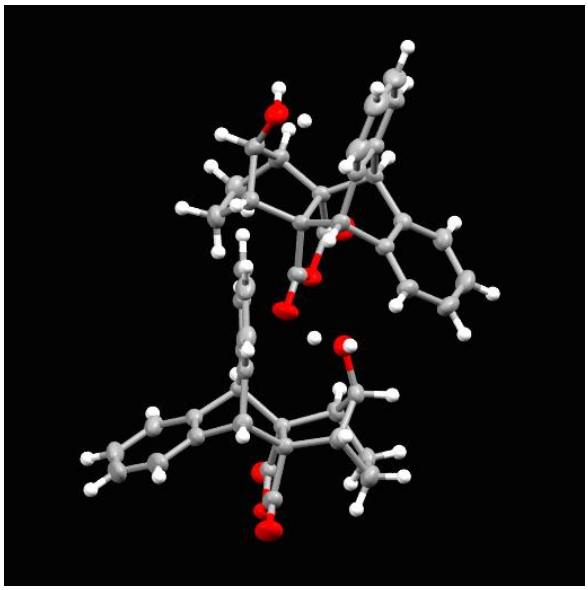

Figure 5. Displacement ellipsoid plot (50% probability level) of 11.

Upon examining an X-ray crystal structure of **11**, we noticed another interesting feature (Figure 5). The oxygen-bound hydrogen atom is disordered over two orientations: the *in*-form is bound to the arene and the *out*-form is involved in a hydrogen bond with the oxygen of an adjacent molecule (encouraged by the rigid positioning of the molecules in the crystal lattice). This result demonstrates the facility by which interconversion can

occur. Note that the *out*-form can be described as a dominant HO—arene interaction, between the lone pairs on oxygen and the arene ring, instead of an OH—arene interaction. In order to study this HO—arene interaction in solution, we envisioned that a more electron deficient arene ring would decrease the favorability of OH—arene hydrogen bonding, so we synthesized **15** and **16** in an analogous fashion to **11** and **14** (Scheme 3), replacing anthracene with 1-trifluoromethylanthracene[96] as the diene. The OH stretching frequencies of **15** and **16** are nearly identical to each other, and to that of nonsubstituted *out*-OH **14**, suggesting that, in contrast to **11**, the hydrogen atom of the OH group of **16** is not hydrogen bound to the arene (a statement that is supported by DFT calculations: see Table 3). In terms of NMR analysis, the OH in **16** is less shielded than **11** by 0.39 ppm. Since the hydrogen atom is facing the other way, it is further from the ring, and thus less affected by ring current shielding.

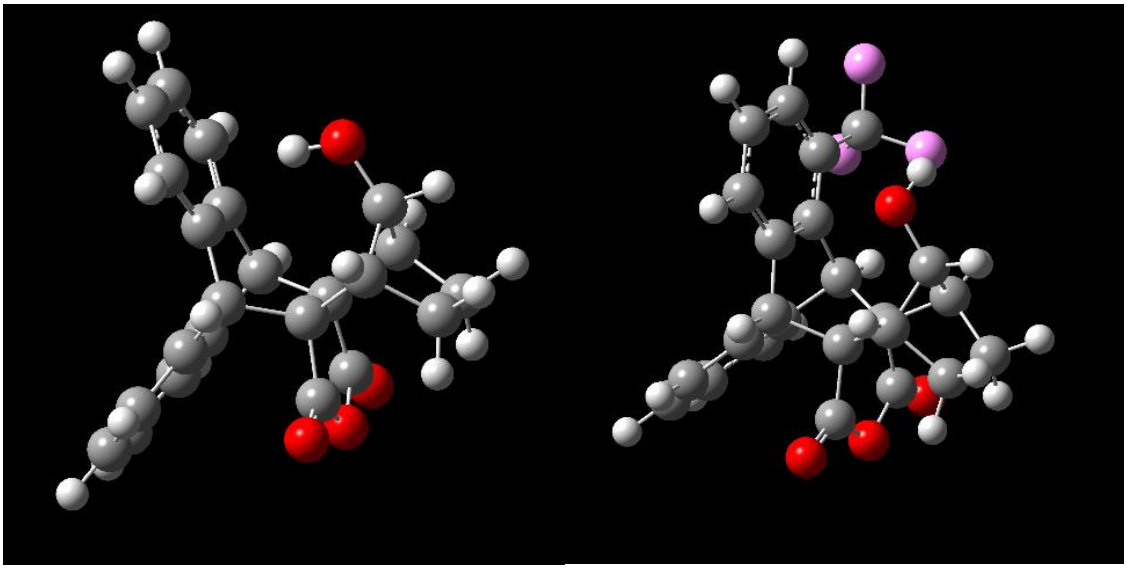

Figure 6. Optimized structures of 11 (left) and 16 (right) (ωB97XD/6-311++G**). Note that the hydroxy-hydrogen faces toward the ring in the case of 1 and away from it in the case of 16.

3.5. Reactivities

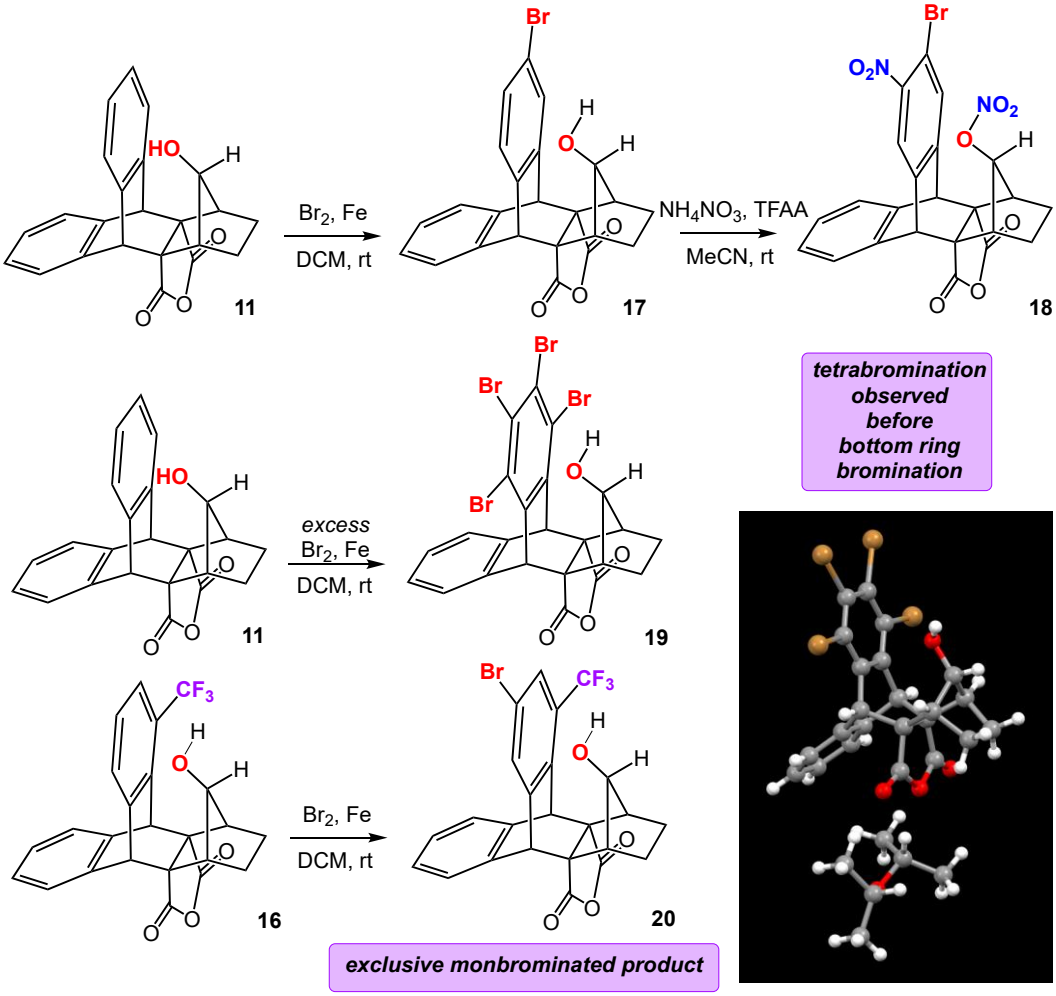

Scheme 4. Reactions of 11, 16, and 17. Bottom Right: Ball and stick model of 19 from crystallographic coordinates. Note that there is an i-Pr_2O solvent molecule in the asymmetric unit.

In application, the OH—arene interaction is expected to be deactivating in an electrophilic aromatic substitution, whereas the HO—arene interaction should be activating. Which effect would dominate in EAS? Monobromination of **11** (Br_2, MeCN, room temperature) forms product **17** exclusively and under exceptionally mild conditions (i.e. without a Lewis acid promoter), confirming that the ring perturbed by the hydroxyl group is activated (Scheme 4).[97,98] Bromine is a moderate electron-withdrawing group that

slows the rate of aromatic substitution by about two orders of magnitude.[99] Taking it one step further, does the HO—arene interaction override this deactivation? We were gratified to find that nitration of **17** also proceeds exclusively on the brominated ring (in addition to nitrate ester formation: Figure 4) (**18**).[100,101] In fact, we found that the nitrate ester forms *prior* to arene nitration (see SI). It is highly noteworthy that even an electron deficient oxygen atom, as part of a nitrate ester, can direct EAS. What is more, when **11** was subjected to more forceful bromination conditions (excess Br_2, Fe metal, CH_2Cl_2), we monitored the reaction and observed tetrabromination of the top ring **19** before any evidence of bottom ring bromination (Figure in Scheme 4 show the crystal structure of **19**).[102,103]

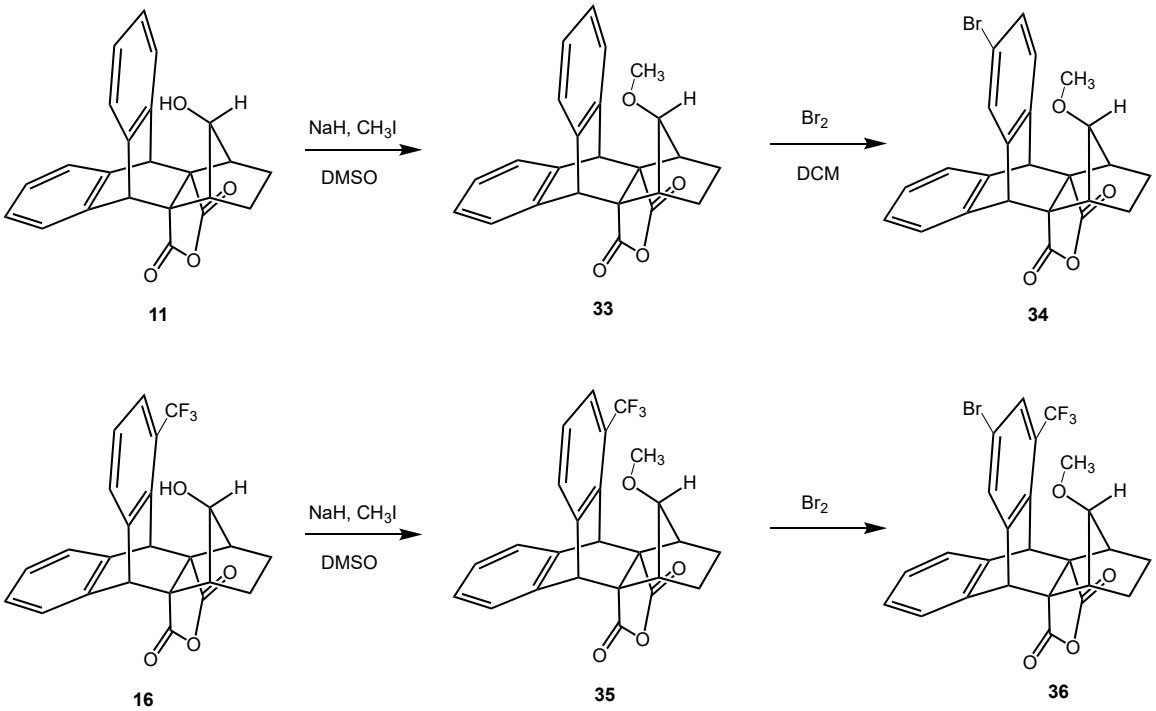

Scheme 5. Synthesis and bromination of 33 and 35.

At this point, we sought a much stronger electron-withdrawing group that would afford a more dramatic demonstration of the external activating effect of the hydroxyl group. One of the most potent deactivators is the trifluoromethyl group, which reduces the relative reactivity of an arene ring by more than 40,000 fold.[104] This significant deceleration also means that any other electron-rich aromatic rings present in a typical synthetic sequence will undergo preferential aromatic substitution under virtually all known conditions. When **16** is subjected to standard bromination conditions at room temperature (Scheme 4) product **20** is obtained (57% yield). The mass balance is composed of starting material and a mixture of polybrominated products. No hint of monobromination on the other aromatic ring was observed, thus demonstrating the hydroxyl group's ability to override one of the strongest deactivating substituents. Additionally, the methyl ether derivatives of **11** and **16** also brominate on the top ring (Scheme 5). In order to attribute these non-traditional substitution patterns to the HO—arene interaction, several control experiments were conducted (Scheme 8).[1] The simplest comparison is between benzene (**21**) and trifluorotoluene (**22**), as no through-space rigid atom—arene interaction would be present.

[1] The *O*-methylated derivatives of **1** and **6** brominate preferentially on the top ring, consistent with activation by the O-atom. See SI for details.

3.6. Control group

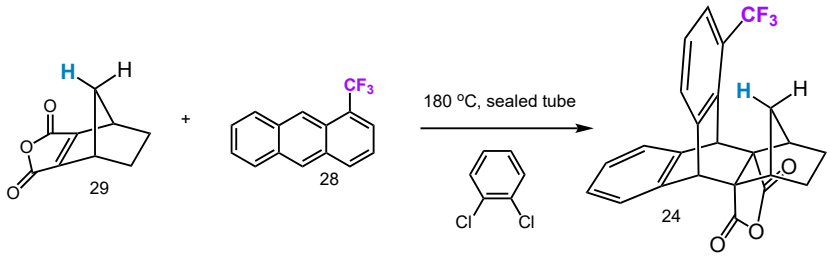

Scheme 6. Synthesis of 24

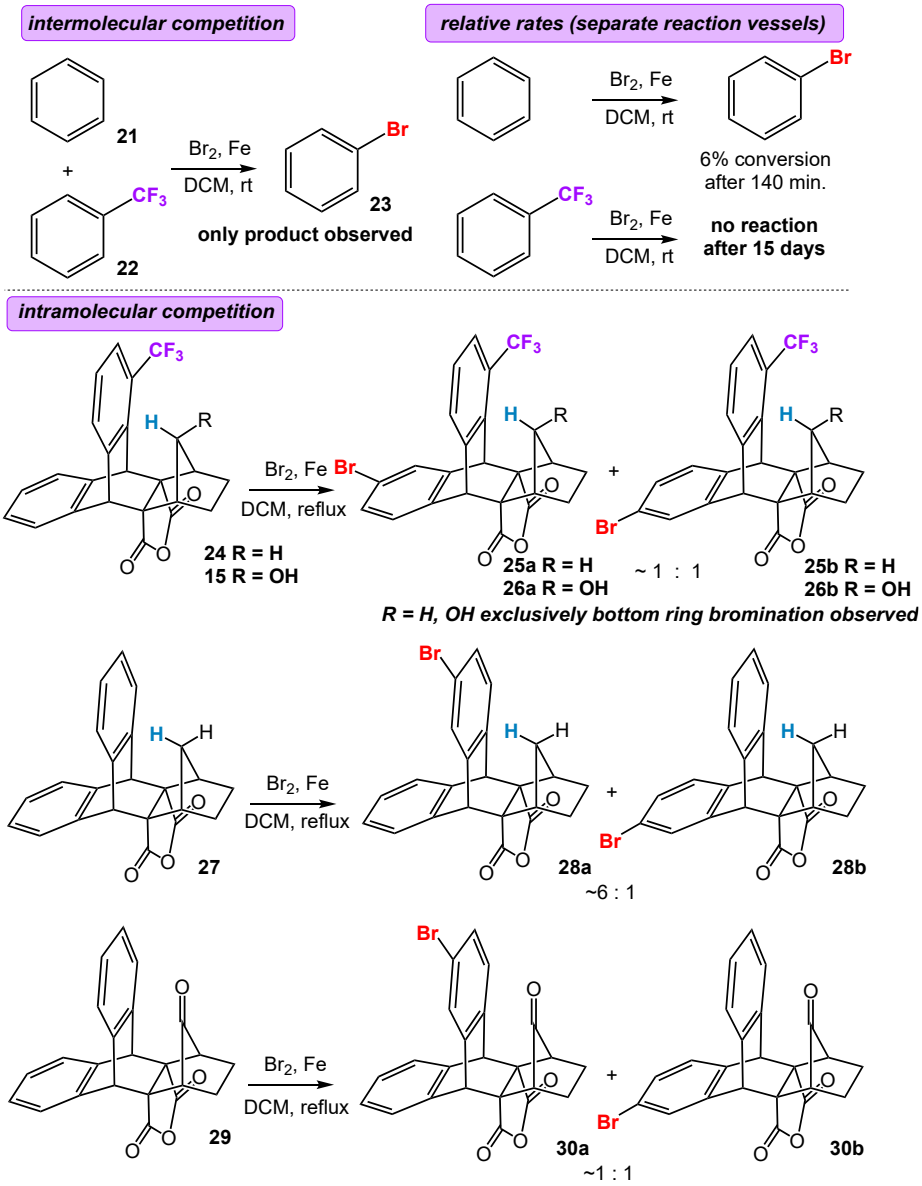

Scheme 7. Control reactions confirming role of HO—arene interaction in through-space activation.

In an intermolecular competitive bromination experiment (with benzene and trifluorotoluene in great excess of other reagents), bromobenzene (**23**) was the only product observed upon complete consumption of Br_2. To illustrate further the relative reaction rates, benzene and trifluorotoluene were subjected to the same bromination conditions in separate vessels. The initial rate of bromobenzene formation was monitored over 140 min. to 6% conversion, while no brominated trifluorotoluene isomers were observed after 15 days. Note that these control reactions were performed under the same conditions whereby **11** underwent rapid bromination, in line with an argument for HO—arene activation. However, criticism of these control experiments may come from the rigidity and substitution pattern of our probe molecule - are there unforeseen features of the framework that *prevent* functionalization of the bottom ring (or otherwise activate the top ring)? Thus, we synthesized **24** (see Scheme 7 and 8),[105] with the hydroxyl group replaced by a less (but still slightly activating) hydrogen atom as an intramolecular control experiment. We also employed out-OH **15** as another control. At room temperature, no bromination was observed after multiple attempts, thus providing initial support for the necessity of the HO—arene activation. Upon refluxing the reaction mixture, bromination was observed exclusively on the bottom ring at the two distal positions in ~1:1 ratio (**25-26a**:**25-26b**). Therefore, the HO—arene activation is crucial in dictating both reactivity and selectivity with regard to this control.

We employed another control molecule, **27**,[59] where there is equal substitution on the aromatic rings, and the hydroxyl group is again replaced with a hydrogen atom (Scheme

8). Bromination of this compound resulted in a mixture of monobromides on the top ring and the bottom ring in a 6:1 ratio. This suggests that the inherent difference in reactivity between the two rings is fairly small on this compound, but that the top ring is still slightly activated by the inward facing hydrogen atom. We would expect this theoretically and in analogy to the profusion of "hydrido-bridged" structures in organic chemistry.[106] Additionally, a slight inherent deactivation of the bottom ring may contribute as well, but the effect is evidently small. This result is in rough accord with previous investigations (nitration of this compound gives a 2:1 ratio of top ring to bottom ring substitution).[59] As a final control, employed ketone **29**, which contains no activating atom. Bromination of **29** resulted in a ~1:1 ratio of top ring to bottom ring products (Scheme 8).

3.7. Computational analysis.

The observed selectivity was further corroborated by DFT calculations. We calculated the relative energies of various σ-complexes leading to potential brominated products of **11**, **16**, **24** and **30** (Table 3). In the case of **11**, the isomer with bromine on the top ring is more stable than that on the bottom ring by 9.0 kcal (ωB97XD/6-311++G**; *exo* bromo slightly more stable than *endo* epimer). This large difference would explain the preferential substitution on the top ring. In the case of **16**, the top ring complex is favored by a lesser amount (3.8 kcal) than in **11**, whereas in the case of **14**, the bottom ring complex is favored by 5.2 kcal.

Table 3. Calculated arenium intermediates.

	A	B	C
11	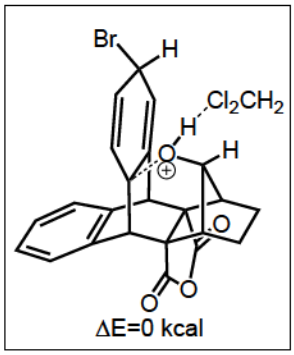 ΔE=0 kcal	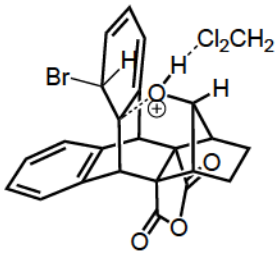 ΔE= 1.92kcal	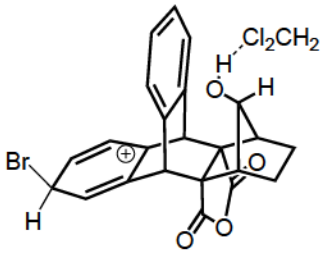 ΔE=9.00 kcal
16	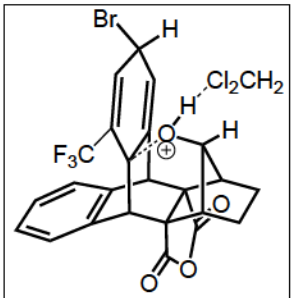 ΔE=0 kcal	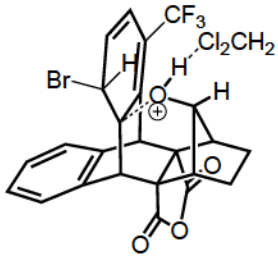 ΔE=8.88 kcal	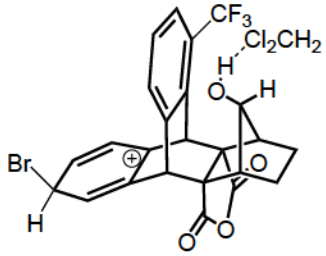 ΔE=3.75 kcal
24	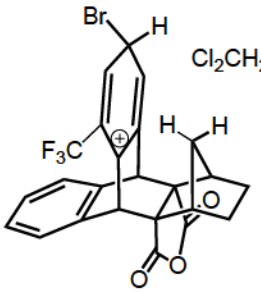 ΔE=0 kcal	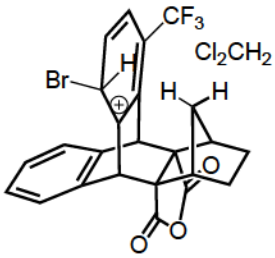 ΔE=5.52 kcal	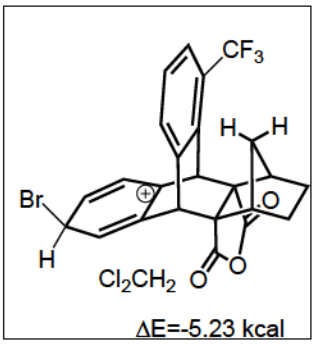 ΔE=-5.23 kcal
30	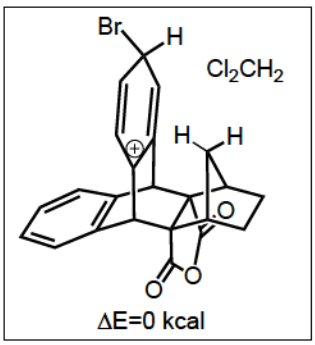 ΔE=0 kcal	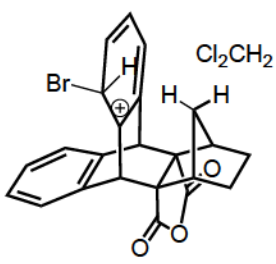 ΔE=4.74 kcal	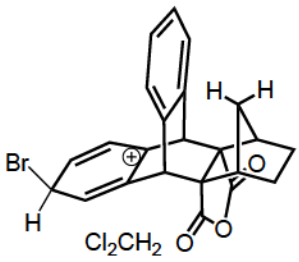 ΔE=2.15 kcal

* For each starting compound, the lowest energy isomer is indicated with a box, and the **A** isomer is used as the reference energy. Note that the **B** isomer is never the lowest energy isomer.

Is the activation truly "Meisenheimer like," i.e., is there a developing covalent bond between oxygen and an arene carbon in the transition state? DFT calculations can shed light on this question using **16** as the model. At ωB97XD/6-311+G**, the σ-complex intermediate **16A** for bromination of **16** was optimized with an explicit solvent molecule (dichloromethane). The oxygen atom in the optimized structure is in close proximity (1.57 Å) to the carbon *ortho* to the trifluoromethyl group and *para* to the complexed bromine (Figure 7).

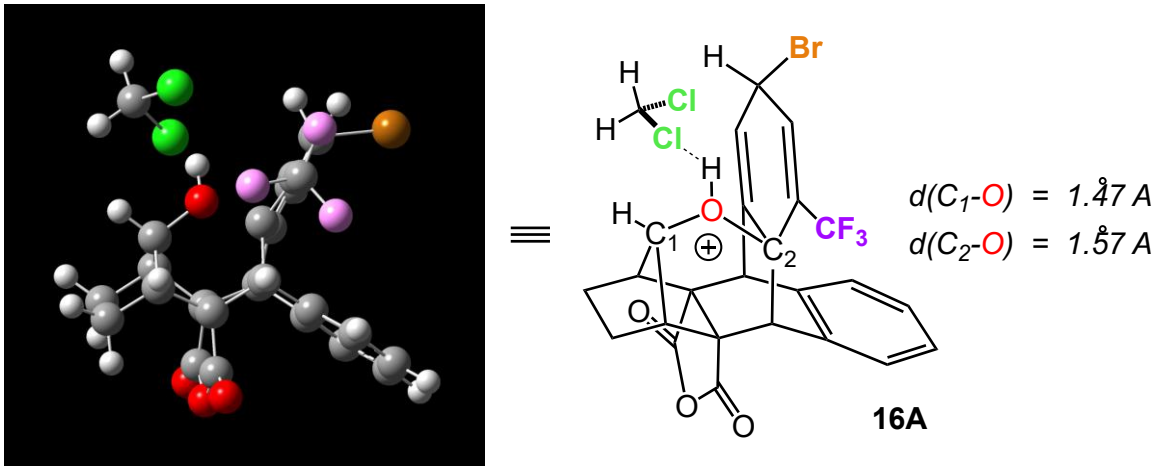

Figure 7. Optimized structure of 16A, the σ-complex intermediate for bromination of 16, at ωB97XD/6-311+G**.

There clearly is a covalent bond between oxygen and the arene carbon atom, which serves to explain the relative stability of this σ-complex compared to those that lead to other products. In addition, an AIM (atoms in molecules) analysis shows the existence of a bond critical point between the oxygen and carbon (Figure 8).[107] Finally, if **16** undergoes exclusive bromination on the top ring (with the trifluoromethyl substituent), is the top ring still considered the more electron-deficient ring in the ground state? Natural bond orbital

(NBO) analyses of the carbon atoms on the aromatic rings show more positive charge character on the trifluoromethylated ring regardless of the presence (**16**) or absence (**24**) of the hydroxyl group (Table 4). Thus, the HO—arene activation must be more influential during the formation of the σ-complex.

Table 4. NBO calculations.

Compound	Ring	Total charge on arene carbon atoms (au)
24	upper	-0.694
24	lower	-0.84
16	upper	-0.637
16	lower	-0.849
11	upper	-0.817
11	lower	-0.856

*NBO calculations.show that the presence of the trifluoromethyl group on the ring makes the sum of the charge of that ring's carbon atoms more positive, while the presence or absence of the OH group exerts a much smaller influence. Perhaps somewhat surprisingly, even in the case of **11**, the upper ring has more positive character.

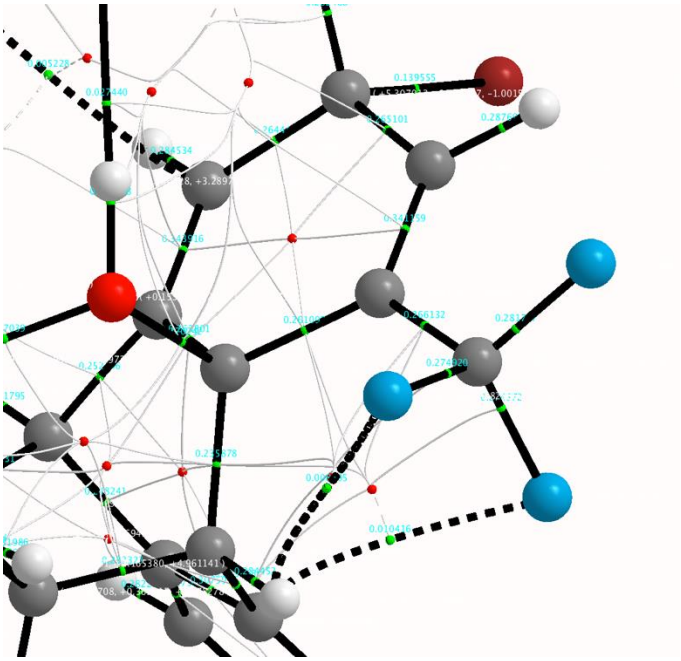

Figure 8. AIM (atoms in molecules) analysis of bromination σ-complex in Figure 16 of main text. Note the bond critical point between the oxygen atom and arene carbon.

3.8. Conclusion

In conclusion, we demonstrated that the HO—aryl interaction dramatically increases an aromatic ring's reactivity with electrophiles such that this phenomenon may override the counterbalance of deactivating substituents. In particular, preferential EAS on a trifluoromethyl-substituted ring over the corresponding unsubstituted aromatic ring is a testament to the strength of this interaction. Not only does this expand the selectivity "rules" of EAS in chemical synthesis based on substituent effects, but it should also draw attention to interactions in, for instance, enzyme active sites where forced HO—arene interactions are plausible.

Chapter 4. Experiment Section

4.1. General Methods.

Unless otherwise stated, all reactions were carried out under strictly anhydrous, air-free conditions under nitrogen. All solvents and reagents were dried and degassed by standard methods. ^{1}H and ^{13}C spectra were acquired on a 400 MHz NMR in $CDCl_3$, $(CD_3)_2CO$, or $(CD_3)_2SO$ at 25 °C; ^{19}F spectra were taken on a 300 MHz NMR in $CDCl_3$, $(CD_3)_2CO$, or $(CD_3)_2SO$ at 25 °C. The ^{1}H, ^{13}C, and ^{19}F chemical shifts are given in parts per million (δ) with respect to an internal tetramethylsilane (TMS, δ 0.00 ppm) standard and/or $CFCl_3$ (δ 0.00 ppm). NMR data are reported in the following format: chemical shifts (multiplicity (s = singlet, d = doublet, t = triplet, q = quartet m = multiplet), integration, coupling constants [Hz]). IR data were obtained using an FT-IR with a flat CaF_2 cell. MS analyses were completed using positive ion mode electrospray ionization (Apollo II ion source) on a Bruker 12.0 Tesla APEX -Qe FTICR-MS. All measurements were recorded at 25 °C unless otherwise stated. Spectral data was processed with ACD/NMR Processor Academic Edition.[2]

4.2. Computational Methods.

The Gaussian '09 package and Spartan '10 were used for all geometry optimizations,[3,4]

[2] ACD/ChemSketch Freeware, Version 12.01, Advanced Chemistry Development, Inc., Toronto, ON, www.acdlabs.com, 2012.

[3] Gaussian '09, Revision A.1, M. J. Frisch, et al. Gaussian, Inc., Wallingford CT, 2009.

[4] Spartan '10 Program, Wavefunction Inc., Irvine, CA.

which were determined using the ωB97XD/6-311++G** level.

4.3. Single Crystal X-ray Crystallography.

4.3.1. Crystal Structure of 11:

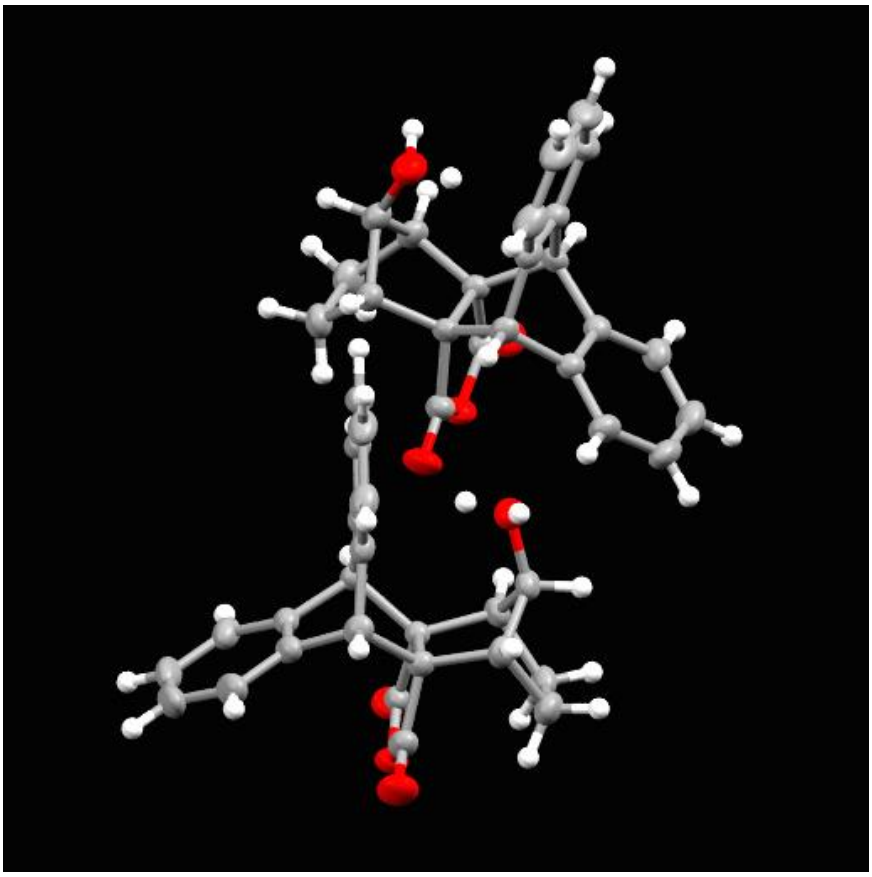

Figure 9. Displacement ellipsoid plot (50% probability level) of 11.

Displacement ellipsoid plot (50% probability level) of 11 displaying two crystallographically independent molecules in the asymmetric unit. The hydroxyl hydrogen atoms are disordered over two orientations – an in-form and an out-form.

All reflection intensities were measured at 250(2) K using a SuperNova diffractometer (equipped with Atlas detector) with Mo $K\alpha$ radiation (λ= 0.71073 Å) under the program CrysAlisPro (Version 1.171.36.32 Agilent Technologies, 2013). The same program was

used to refine the cell dimensions and for data reduction. The structure was solved with the program SHELXS-2014/7 (Sheldrick, 2015) and was refined on F^2 with SHELXL-2014/7 (Sheldrick, 2015). Numerical absorption correction based on gaussian integration over a multifaceted crystal model was applied using CrysAlisPro. The temperature of the data collection was controlled using the system Cryojet (manufactured by Oxford Instruments). The H atoms were placed at calculated positions (unless otherwise specified) using the instructions AFIX 13, AFIX 23 or AFIX 43 with isotropic displacement parameters having values 1.2 *U*eq of the attached C atoms. The H atoms attached to O1A and O1B are found to be disordered over two orientations. As O1A (and O1B) is H-bond donor in one intermolecular hydrogen bond interaction, disorder must occur as there would be impossible short H…H contacts in the solid state otherwise. The O1X–H1X1 (X = A, B) bonds participate in the intermolecular O–H…O hydrogen bond interactions. The O1X–H1X2 and O1X–H1X2 are oriented toward the C18X→C23X (X = A, B). The occupancy factors between the major and minor components of the disorder are statistically equal to 0.5 (within standard uncertainties).

Additional notes:

(i) There are two crystallographically independent molecules in the asymmetric unit (Z' = 2).

(ii) Significant crystal damages occur when the crystals are flash cooled to 110, 150, 200, 220 K, most likely due to a destructive solid-solid phase transition. At 250 K, the crystal

integrity remains stable.

Crystallographic experimental details.

Compound	**11**
Crystal data	
Chemical formula	$C_{23}H_{18}O_4$
M_r	358.37
Crystal system, space group	Monoclinic, $P2_1/c$
Temperature (K)	250
a, b, c (Å)	14.9116 (5), 10.7633 (4), 21.0691 (7)
β (°)	92.606 (3)
V (Å^3)	3378.1 (2)
Z	8
Radiation type	Mo $K\alpha$
μ (mm^{-1})	0.10
Crystal size (mm)	0.55 × 0.37 × 0.33
Data collection	
Diffractometer	SuperNova, Dual, Cu at zero, Atlas
Absorption correction	Gaussian *CrysAlis PRO*, Agilent Technologies, Version 1.171.36.32 (release 02-08-2013 CrysAlis171 .NET) (compiled Aug 2 2013,16:46:58) Numerical absorption correction based on gaussian integration over a multifaceted crystal model
T_{min}, T_{max}	0.417, 1.000
No. of measured, independent and observed [$I > 2\sigma(I)$] reflections	26536, 7740, 6087

R_{int}	0.028
$(\sin \theta/\lambda)_{max}$ (Å^{-1})	0.650
Refinement	
$R[F^2 > 2\sigma(F^2)]$, $wR(F^2)$, S	0.046, 0.121, 1.03
No. of reflections	7740
No. of parameters	501
No. of restraints	4
H-atom treatment	H atoms treated by a mixture of independent and constrained refinement
$\Delta\rho_{max}$, $\Delta\rho_{min}$ (e Å^{-3})	0.30, -0.25

Computer programs: *CrysAlis PRO*, Agilent Technologies, Version 1.171.36.32 (release 02-08-2013 CrysAlis171 .NET) (compiled Aug 2 2013, 16:46:58), *SHELXS2014*/7 (Sheldrick, 2015), *SHELXL2014*/7 (Sheldrick, 2015), *SHELXTL* v6.10 (Sheldrick, 2008).[5]

[5] Sheldrick, G. M. *Acta Cryst.* **2015,** *C71*, 3-8.

4.3.2. Crystal Structure of 18:

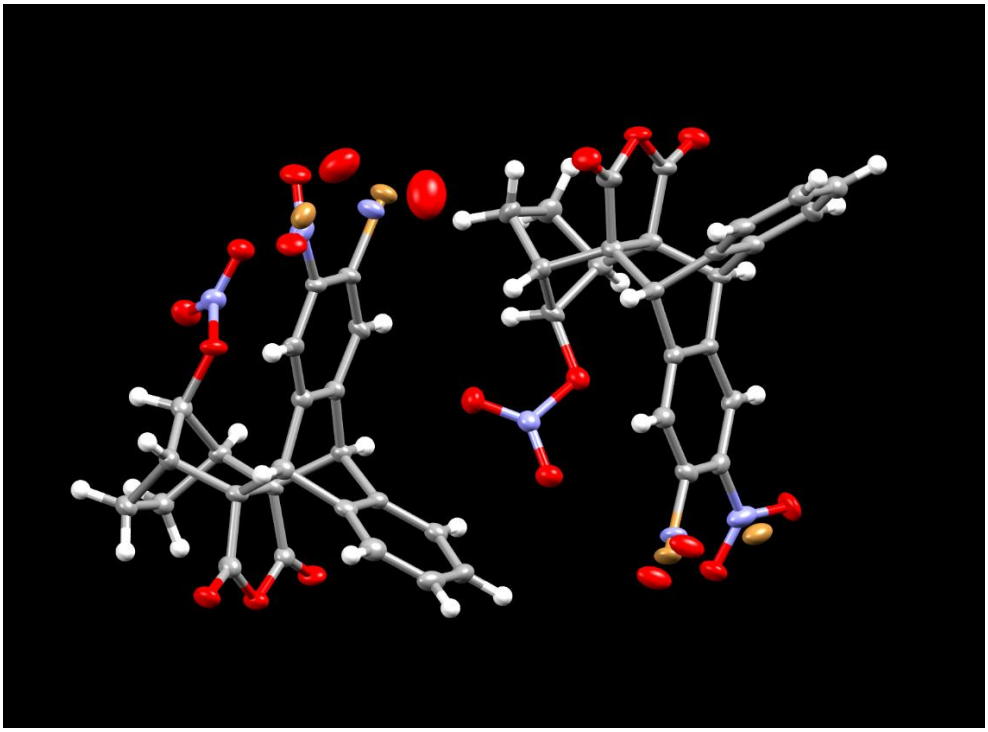

Figure 10. Displacement ellipsoid plot (50% probability level) of 18.

Displacement ellipsoid plot (50% probability level) of **18** displaying two crystallographically independent molecules in the asymmetric unit. The bromo and nitro substituents are disordered (the minor component of the disorder is shown as non connected atoms) over two positions, as the compound exists as a racemic mixture of enantiomers.

All reflection intensities were measured at 110(2) K using a SuperNova diffractometer (equipped with Atlas detector) with Cu *K*α radiation (λ = 1.54178 Å) under the program CrysAlisPro (Version 1.171.36.32 Agilent Technologies, 2013). The same program was used to refine the cell dimensions and for data reduction. The structure was solved with the program SHELXS-2014/7 (Sheldrick, 2015) and was refined on F^2 with SHELXL-2014/7 (Sheldrick, 2015). Analytical numeric absorption correction using a multifaceted crystal

model was applied using CrysAlisPro. The temperature of the data collection was controlled using the system Cryojet (manufactured by Oxford Instruments). The H atoms were placed at calculated positions (unless otherwise specified) using the instructions AFIX 13, AFIX 23 or AFIX 43 with isotropic displacement parameters having values 1.2 or 1.5 *U*eq of the attached C atoms. The structure is partly disordered.

The asymmetric contains two crystallographically independent molecules ($Z' = 2$) that are mostly ordered, except for the positional disorder of –Br/–NO_2. All occupancy factors can be retrieved in the *.cif* file.

When running the *.cif* file *via* PLATON/CheckCIF, the ADDSYM procedure (2 Alerts B) strongly suggests the space group $P2_1/n$ with $Z' = 1$. While refining the structure in the $P2_1/n$, the statistics were significantly worse (higher R1 and wR2 factor of 5.6% and 15.3%, respectively and the analysis of variance suggested unusually high K values) than in *Pn*. A look at the digitally reconstructed reciprocal lattices 0*kl* and *hk*0 shows that not all 0*k*0 reflections (when *k* is odd) are systematically absent, suggesting that there is no true 2_1 screw axis along the **b** direction. The space group *Pn* with Z' = 2 was preferred, and refinement statistics in this space group dramatically improved (see table 1).

The checkCIF procedure also suggests potential intermolecular hydrogen bonding:

430_ALERT_2_B Short Inter D...A Contact O1A .. O3B .. 2.79 Ang.

430_ALERT_2_B Short Inter D...A Contact O2B .. O3A .. 2.79 Ang.

Those alerts are concerned with the nitrate ester groups, but those groups cannot be

protonated at the positions: O1X/O2X, X = A, B as the N-O distances are *ca.* 1.2 Å.

The structure was refined as an inversion twin, and the Flack parameter refines to 0.22(2)

Crystallographic experimental details.

Compound	**18**
Crystal data	
Chemical formula	$C_{23}H_{15}BrN_2O_8$
M_r	527.28
Crystal system, space group	Monoclinic, *Pn*
Temperature (K)	110
a, *b*, *c* (Å)	14.14437 (18), 10.66001 (10), 14.34156 (18)
β (°)	115.5506 (16)
V (Å^3)	1950.93 (5)
Z	4
Radiation type	Cu *K*α
μ (mm^{-1})	3.42
Crystal size (mm)	0.22 × 0.17 × 0.12
Data collection	
Diffractometer	SuperNova, Dual, Cu at zero, Atlas
Absorption correction	Analytical *CrysAlis PRO*, Agilent Technologies, Version 1.171.36.32 (release 02-08-2013 CrysAlis171 .NET) (compiled Aug 2 2013,16:46:58) Analytical numeric absorption correction using a multifaceted crystal model based on expressions derived by R.C. Clark & J.S. Reid. (Clark, R. C. & Reid, J. S. (1995). Acta Cryst. A51, 887-897)
T_{min}, T_{max}	0.617, 0.741
No. of measured, independent and observed [$I > 2\sigma(I)$] reflections	22369, 6422, 6199
R_{int}	0.024
$(\sin\theta/\lambda)_{max}$ (Å^{-1})	0.616
Refinement	
$R[F^2>2\sigma(F^2)]$,	0.032, 0.090, 1.06

$wR(F^2)$, S	
No. of reflections	6422
No. of parameters	658
No. of restraints	153
H-atom treatment	H-atom parameters constrained
$\Delta\rho_{max}$, $\Delta\rho_{min}$ (e Å^{-3})	0.59, -0.44
Absolute structure	Refined as an inversion twin.
Absolute structure parameter	0.22 (2)

Computer programs: *CrysAlis PRO*, Agilent Technologies, Version 1.171.36.32 (release 02-08-2013 CrysAlis171 .NET) (compiled Aug 2 2013, 16:46:58), *SHELXS2014*/7 (Sheldrick, 2015), *SHELXL2014*/7 (Sheldrick, 2015), *SHELXTL* v6.10 (Sheldrick, 2008).[5]

4.3.3. Crystal Structure of 19:

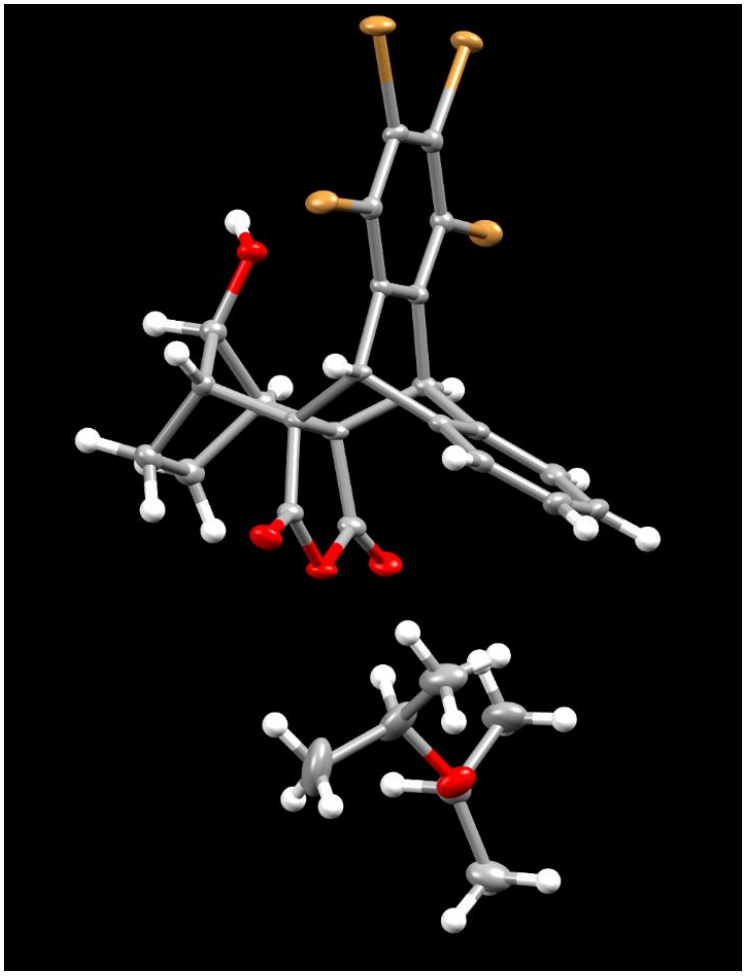

Figure 11. Displacement ellipsoid plot (50% probability level) of 19 with diisopropyl ether solvent molecule in the asymmetric unit.

All reflection intensities were measured at 110(2) K using a SuperNova diffractometer (equipped with Atlas detector) with Cu *K*α radiation (λ = 1.54178 Å) under the program CrysAlisPro (Version 1.171.36.32 Agilent Technologies, 2013). The same program was used to refine the cell dimensions and for data reduction. The structure was solved with the program SHELXS-2014/7 (Sheldrick, 2015) and was refined on F^2 with SHELXL-2014/7 (Sheldrick, 2015). Analytical numeric absorption correction using a multifaceted crystal

model was applied using CrysAlisPro. The temperature of the data collection was controlled using the system Cryojet (manufactured by Oxford Instruments). The H atoms were placed at calculated positions (unless otherwise specified) using the instructions AFIX 13, AFIX 23, AFIX 43 or AFIX 137 with isotropic displacement parameters having values 1.2 or 1.5 *U*eq of the attached C atoms. The H atom attached to O1 was found from difference Fourier map, and its coordinates and isotropic temperature factor were refined freely (the O–H bond distance was restrained to be 0.84(3) Å using the DFIX instruction). The structure is ordered.

Specified hydrogen bonds (with esds except fixed and riding H)

D-H	H...A	D...A	<(DHA)	
0.83(3)	1.92(3)	2.739(3)	171(4)	O1-H1A...O1S_$2

Crystallographic experimental details.

Compound	**19**
Crystal data	
Chemical formula	$C_{23}H_{14}Br_4O_4 \cdot C_6H_{14}O$
M_r	776.15
Crystal system, space group	Triclinic, *P*-1
Temperature (K)	110
a, *b*, *c* (Å)	9.0304 (3), 10.5730 (3), 15.5426 (5)
α, β, γ (°)	98.576 (3), 91.662 (3), 104.927 (3)
V (Å^3)	1414.34 (8)
Z	2
Radiation type	Cu *K*α

μ (mm^{-1})	7.26
Crystal size (mm)	0.11 × 0.07 × 0.03
Data collection	
Diffractometer	SuperNova, Dual, Cu at zero, Atlas
Absorption correction	Analytical *CrysAlis PRO*, Agilent Technologies, Version 1.171.36.32 (release 02-08-2013 CrysAlis171 .NET) (compiled Aug 2 2013,16:46:58) Analytical numeric absorption correction using a multifaceted crystal model based on expressions derived by R.C. Clark & J.S. Reid. (Clark, R. C. & Reid, J. S. (1995). Acta Cryst. A51, 887-897)
T_{min}, T_{max}	0.572, 0.843
No. of measured, independent and observed [$I > 2\sigma(I)$] reflections	18258, 5514, 4817
R_{int}	0.034
$(\sin \theta/\lambda)_{max}$ ($Å^{-1}$)	0.616
Refinement	
$R[F^2>2\sigma(F^2)]$, $wR(F^2)$, S	0.029, 0.071, 1.03
No. of reflections	5514
No. of parameters	351
No. of restraints	1
H-atom treatment	H atoms treated by a mixture of independent and constrained refinement
$\Delta\rho_{max}$, $\Delta\rho_{min}$ (e $Å^{-3}$)	0.75, -0.56

Computer programs: *CrysAlis PRO*, Agilent Technologies, Version 1.171.36.32 (release 02-08-2013 CrysAlis171 .NET) (compiled Aug 2 2013, 16:46:58), *SHELXS2014*/7 (Sheldrick, 2015), *SHELXL2014*/7 (Sheldrick, 2015), *SHELXTL* v6.10 (Sheldrick, 2008).[5]

4.4. Compound Characterization.

^{1}H NMR and ^{13}C NMR: the known chemical shift[6] of residual solvent signal is used as secondary references. ^{19}F NMR: the chemical shift of $CFCl_3$ is used as references.

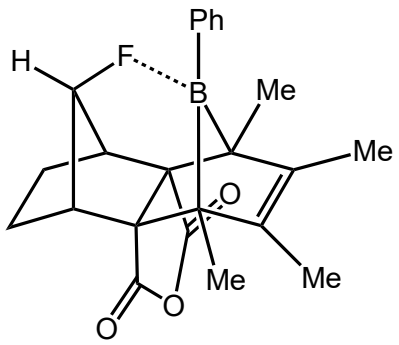

12-fluoro-1,2,3,4-tetramethyl-13-phenyl-1,4,5,6,7,8-hexahydro-1,4-borano-5,8-methano-4a,8a-(methanooxymethano)naphthalene-9,11-dione (4). To a sealed tube was added freshly made dimer **1** (0.971 g, 2.48 mmol) dissolved in 3 mL dry, degassed DCM and dienophile **3** (0.903, 4.96 mmol). The tube was sealed and heated at 80 ºC for six hours. The solvent was removed in vaccuo and the crude product was purified by flash column chromatography on Florisil with a 5% ethyl acetate and hexanes solution to yield **4** as white crystals (0.8426 g, 45 % yield); ^{1}H NMR ($CDCl_3$) δ 7.26-7.20 (m, 3H), 7.18-7.09 (m, 2H), 5.11 (d, 1H, J = 56.7 Hz), 2.96 (m, 2H), 1.88 (m, 6H), 1.82 (d, 2H, J = 8.8 Hz), 1.48 (s, 6H), 1.42 (m, 2 H); ^{13}C NMR ($CDCl_3$) 172.97 (J = 0.7 Hz), 133.58, 133.55, 130.96 (J = 2.6 Hz), 127.99, 127.66, 103.47 (J = 206.03 Hz), 72.96 (J = 4.8 Hz), 42.12 (J = 15.5 Hz), 21.55, 21.44, 12.05, 11.46; ^{19}F NMR ($CDCl_3$) -189.12 (d, 1F,

[6]Fulmer, G. R.; Miller, A. J. M.; Sherden, N. H.; Gottlieb, H. E.; Nudelman, A.; Stoltz, B. M.; Bercaw, J. E.; Goldberg, K. I. *Organometallics* **2010**, *29*, 2176-2179.

J = 56.79 Hz).

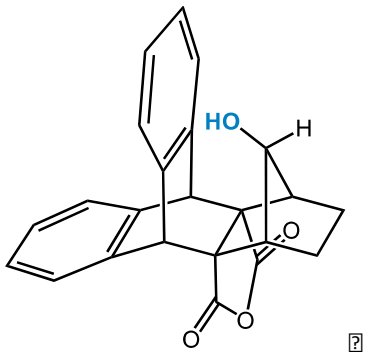

15-hydroxy-9,10-dihydro-9,10-[4,7]methanoisobenzofurano-anthracene-12,14-dione (1). Compound **29** (0.29g, 0.81 mmol) was added to a flame-dried round-bottom flask with 10 mL DCM, followed by 0.87 mL of 1M $LiAlH_4$ in THF. After stirring at room temperature for 2 h under N_2, the reaction was quenched with 0.05 mL water, then was added 0.1 mL 10% NaOH solution, and 0.15 mL water. The mixture was stirred for 15 min, then filtered, dried with $MgSO_4$, concentrated under reduced pressure and purified by silica gel chromatography with a 40% ethyl acetate and hexanes solution. Product **11** was isolated as white crystals (0.20 g, 0.56 mmol, 69.1% yield). ^{1}H NMR ($CDCl_3$) δ 7.50-7.44 (m, 2H), 7.31-7.25 (m, 4H), 7.19-7.13 (m, 2H), 4.78 (s, 2H), 3.85 (d, 1H, J = 10.8 Hz), 2.54 (s, 2H), 1.85-1.79 (m, 2H), 1.41-1.35 (m, 2H), -0.22 (d, 1H, J = 10.9); ^{13}C NMR ($(CD_3)_2CO$) δ 174.27, 143.27, 143.09, 127.75, 127.37, 126.30, 126.13, 84.94, 69.35, 49.72, 47.04, 25.78; IR 3578, 3071, 2982, 2961, 2906, 1851, 1777 (cm^{-1}, CaF_2, CH_2Cl_2); HRMS (ESI-) calc for $C_{23}H_{17}O_4$-: 357.1132 found 357.1134.

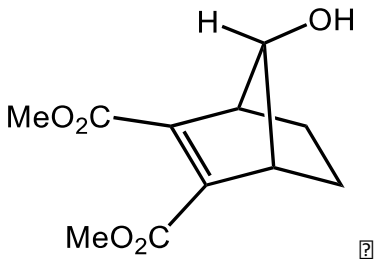

Dimethyl 7-hydroxybicyclo[2.2.1]hept-2-ene-2,3-dicarboxylate (12). Target molecule was synthesized by following the synthetic route found in the literature. Spectral and analytical data were in agreement with previous reports.[7]

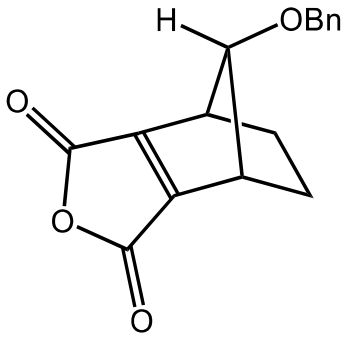

8-(benzyloxy)-4,5,6,7-tetrahydro-4,7-methanoisobenzofuran-1,3-dione (13). Compound **12** (6.00 g, 26.52 mmol) and benzyl 2,2,2-trichloroacetimidate (8.04 g, 31.83 mmol) were dissolved in 20 mL of DCM in an ice water bath. Then TfOH (0.12 mL, 1.33 mmol) was added to the solution. After stirring for 3 h, the reaction was quenched with saturated $NaHCO_3$ solution (10 mL). The resulting mixture was extracted with DCM (3 x 20 mL), dried with $MgSO_4$, and concentrated under reduced pressure. The crude product was purified by silica gel chromatography with a 10% ethyl acetate and hexanes solution. The product from the previous step was dissolved in 30 mL of THF, and an aqueous LiOH

[7] Holl, M. G.; Struble, M. D.; Singal, P.; Siegler, M. A.; Lectka, T. *Angew. Chem. Int. Ed.* **2016,** *55,* 8266-8269.

solution (3.67 g in 30 mL of water) was added. The reaction was stirred for 3 h at room temperature, then acidified with concentrated HCl and extracted with ethyl acetate (4 x 20 mL). The organic fractions were combined, dried with $MgSO_4$ and concentrated under reduced pressure.

The crude product was dissolved with 10 mL of trifluoroacetic anhydride (TFAA) and stirred for 2 h at room temperature. Then, the solution was concentrated *in vacuo.* Product **13** can be purified by recrystallization from pentane/Et_2O (3.00 g, 11.10 mmol, 41.9% yield); ^1H NMR ($CDCl_3$) δ 7.40-7.28 (m, 5H), 4.52 (s, 2H), 3.65 (s, 1H), 3.31 (m, 2H), 2.30-2.24 (m, 2H), 1.27-1.21 (m, 2H); ^{13}C NMR ($CDCl_3$) δ 160.27, 155.35, 137.18, 128.77, 128.36, 127.81, 91.64, 71.76, 43.31, 22.74; HRMS (ESI+) calc for $C_{16}H_{14}O_4Na^+$: 293.0784, found 293.0785.

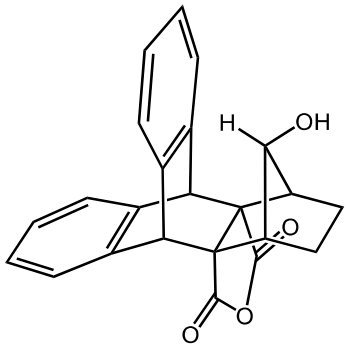

15-hydroxy-9,10-dihydro-9,10-[4,7]methanoisobenzofurano-anthracene-12,14-dione (14). In a sealed glass pressure vessel were combined **13** (0.40 g, 1.48 mmol), anthracene (0.79 g, 4.44 mmol) and 1,2-dichlorobenzene (3.5 mL). The vessel was then sealed and heated to 160 °C for two days. The crude product was purified by silica gel flash column chromatography, first with hexanes to remove anthracene, then with a 20% ethyl acetate and hexanes solution to elute the product.

The product was dissolved in a mixture of 20 mL THF and 20 mL MeOH, with a catalytic amount of Pd/C. A H_2 balloon was connected and the mixture was let to stir overnight. The crude product was purified by silica gel chromatography with a 30% ethyl acetate and hexanes solution. **14** was isolated as a white solid (0.23 g, 0.64 mmol, 43% yield); ^{1}H NMR ($CDCl_3$) δ 7.40-7.33 (m, 2H), 7.30-7.25 (m, 2H), 7.24-7.20 (m, 2H), 7.19-7.13 (m, 2H), 4.66 (s, 2H), 2.52 (s 1H), 2.40 (m, 2H), 2.07-2.01 (m, 2H), 1.39-1.33 (m, 2H), 1.16(s, 1H); ^{13}C NMR ($CDCl_3$) δ 172.76, 140.90, 139.80, 127.79, 127.73, 125.41, 125.33, 63.92, 49.14, 46.42, 24.14; IR 3609, 3071, 2971, 2903, 1848, 1780 (cm^{-1}, CaF_2, CH_2Cl_2); HRMS (ESI-) calc for $C_{23}H_{17}O_4$-: 357.1132 found 357.1135.

15 **15-down**

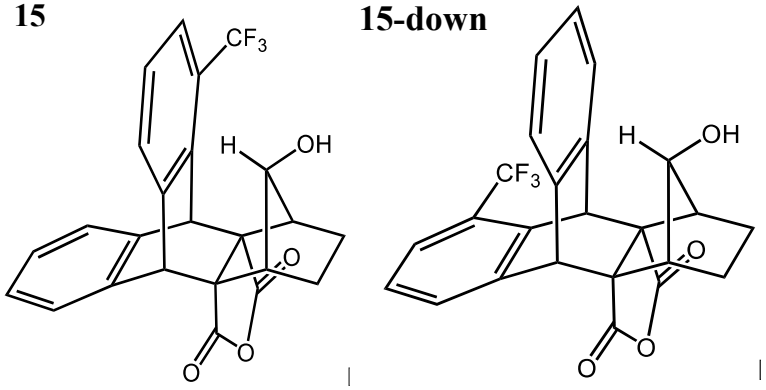

15-hydroxy-4-(trifluoromethyl)-9,10-dihydro-9,10-[4,7]methanoisobenzofuranoanthracene-12,14-dione (15) and **15-hydroxy-4-(trifluoromethyl)-9,10-dihydro-9,10-[4,7]methanoisobenzofurano anthracene-12,14-dione (15-down).** In a sealed glass pressure vessel with stir bar were combined **13** (1.12 g, 4.13 mmol), 1-(trifluoromethyl)anthracene (0.80 g, 3.25 mmol) and 1,2-dichlorobenzene (5 mL). The vessel was then sealed and heated to 180 °C for 24 h with stirring. The crude product was purified by silica gel flash column chromatography with a 20% ethyl acetate and hexanes solution.

Then the product from the previous step was dissolved in a mixture of 20 mL THF and 20 mL MeOH, with catalytic Pd/C. A H_2 balloon was connected to provide H_2 and the mixture was stirred overnight. The crude product was purified by silica gel chromatography with 30% ethyl acetate and hexanes solution. **15** and **15-down** were collected as a mixture (0.84 g, 1.97 mmol 60.6% yield); ^{1}H NMR ($CDCl_3$) δ 7.57 (d, 2H, J = 7.9 Hz), 7.40-7.29 (m, 3H), 7.24-7.19 (m, 2H), 5.18 (s, 1H), 4.76 (s, 1H), 2.55 (s, 1H), 2.51 (s, 1H), 2.44 (s, 1H), 2.08-2.02 (m, 2H), 1.40-1.34 (m, 2H), 1.23 (s, 1H); ^{13}C NMR ($CDCl_3$) δ 172.35, 172.10,

143.24, 139.77 (q, J = 1.9 Hz), 139.29, 138.58, 128.64, 128.25, 128.23, 127.54, 125.84, 125.50, 124.22 (q, J = 5.21 Hz), 63.61, 63.41, 49.04, 46.58, 46.12, 45.65 (q, J = 1.67 Hz), 24.13, 24.07; ^{19}F NMR ($CDCl_3$) δ -59.21 (s, 1F); IR 3609, 2975, 2902, 1844, 1780 (cm^{-1}, CaF_2, CH_2Cl_2); HRMS (ESI-) calc for $C_{24}H_{17}F_3O_4Na^+$: 449.097115 found 449.096871.

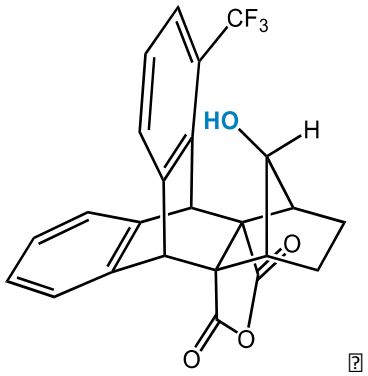

15-hydroxy-4-(trifluoromethyl)-9,10-dihydro-9,10-[4,7]methanoisobenzofuranoanthracene-12,14-dione (16). To a 100-mL round-bottom flask equipped with a condenser were added **15** (0.10 g, 0.23 mmol), crushed 4 Å molecular sieves (1.20 g), and K_2CO_3 (0.60 g). To the mixture was added DCM (30 mL) followed by PCC (0.15 g, 0.69 mmol). The solution was refluxed for 4 h. The mixture was concentrated under reduced pressure and then purified by silica gel flash chromatography with a 20% ethyl acetate and hexanes solution.

The product from the previous step was added to a flame-dried round bottom flask with 10 mL DCM, followed by 0.35 mL of 1 M $LiAlH_4$ in THF. After stirring at room temperature for 2 h under N_2 atmosphere, the reaction was quenched with 0.02 mL water, then was added 0.04 mL 10% NaOH solution, and 0.06 mL water. The mixture was stirred for 15 min, then filtered, dried with $MgSO_4$, concentrated under reduced pressure and purified by silica gel chromatography with a 40% ethyl acetate and hexanes solution. Further purification by preparatory HPLC separated **16** from the *down* isomer, yielding **16** as white crystals (0.06 g, 0.14 mmol, 61% yield). ^{1}H NMR ($(CD_3)_2CO$) δ 7.56 (d, 1H, J = 7.50 Hz),

7.36-7.26 (m, 3H), 7.21-7.14 (m, 3H), 5.10 (s, 1H), 4.95 (s, 1H), 4.02 (d, 1H, J = 4.85 Hz), 2.50 (s, 1H), 2.44 (s, 1H), 1.89-1.83 (m, 2H), 1.28-1.22 (m, 2H); ^{13}C NMR ($(CD_3)_2CO$) δ 174.07, 174.05, 145.82, 143.14, 142.07 (q, J = 2.28 Hz), 142.03, 129.69, 128.25, 128.09, 126.79, 126.35, 126.31, 123.25, 123.20, 123.23 (q, J = 5.02 Hz), 84.27, 68.85, 68.71, 49.67, 47.13, 46.90, 46.80, 25.60, 25.51; ^{19}F NMR ($(CD_3)_2CO$) δ -58.29 (s, 1F); IR 3606, 2905, 1844, 1779 (cm^{-1}, CaF_2, CH_2Cl_2); HRMS (ESI-) calc for $C_{24}H_{16}F_3O_4$-: 425.1006 found 425.1008.

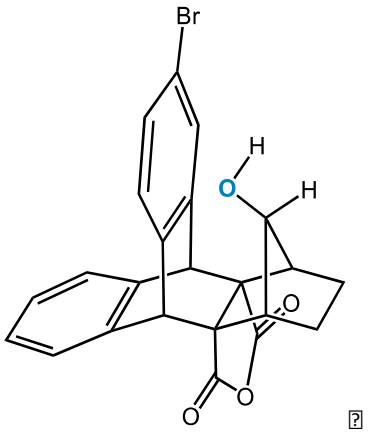

3-bromo-15-hydroxy-9,10-dihydro-9,10-[4,7]methano-isobenzofuranoanthracene-12,14-dione (17). 11 (0.18 g, 0.50 mmol) was dissolved in 10 mL CH_3CN in a 25-mL round-bottom flask, then was added Br_2 (0.065 mL, 1.25 mmol), The reaction was allowed to stir at room temperature for 5 h. The mixture was concentrated under reduced pressure and then purified by silica gel chromatography with a 30% ethyl acetate and hexanes solution. Product **17** was isolated as white crystal (0.16g, 0.37mmol, 74.0% yield). ^{1}H NMR ($CDCl_3$) δ 7.52 (d, 1H, J =1.56 Hz), 7.32 (dd, 1H, J^1 =7.96 Hz, J^2=1.85 Hz), 7.29-7.21 (m, 3H), 7.19-7.13 (m, 2H), 4.73 (s, 1H), 4.70 (s, 1H), 3.94 (d, 1H, J =7.32 Hz), 2.54 (s, 1H), 1.86-1.80 (m, 2H), 1.42-1.36 (m, 2H), 0.15 (d, 1H, J =7.47 Hz); ^{13}C NMR ($(CD_3)_2SO$) δ 173.44, 144.93, 142.02, 141.78, 141.73, 128.03, 127.58, 126.90, 126.86, 126.68, 125.16, 125.07, 118.26, 82.62, 67.78, 67.76, 47.53, 45.56, 45.49, 24.44; HRMS (ESI-) calc for $C_{23}H_{16}O_4Br$-: 435.0237, found 435.0238.

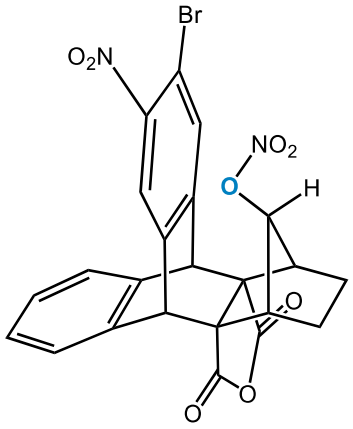

3-bromo-2-nitro-12,14-dioxo-9,10-dihydro-9,10-[4,7]methanoisobenzofuranoanthracen-15-yl nitrate (18). To a 100-mL round-bottom flask were added **17** (0.015 g, 0.034 mmol), and NH_4NO_3 (0.006 g, 0.072 mmol). To the mixture was added CH_3CN (5 mL) and the mixture was cooled to -10 °C in an ice-acetone bath, then was added TFAA (trifluoroacetic anhydride, cat.). The reaction was allowed warm back to room temperature and stirred for 4 h, then quenched with water and extracted with DCM (2 x 10 mL). The organic fractions were combined, dried with $MgSO_4$ and concentrated under reduced pressure. The crude product was further purified by silica gel chromatography with 30% ethyl acetate and hexanes solution. Product **18** yields as white crystals (0.013 g, 0.025 mmol, 73.5% yield). ^{1}H NMR ($(CD_3)_2CO$) δ 8.07 (s, 1H), 7.95 (s, 1H), 7.35-7.38 (m, 2H), 7.23-7.26 (m, 2H), 5.18 (s, 1H), 5.14 (s, 1H), 5.07 (s, 1H), 3.09 (s, 2H), 2.14-2.20 (m, 2H), 1.49-1.55 (m,2H); ^{13}C NMR ($(CD_3)_2CO$) δ 172.60, 172.58, 147.95, 142.93, 141.46, 140.96, 132.30, 128.80, 128.79 126.92, 126.79, 123.45, 114.07, 90.97, 68.41, 68.39, 48.44, 48.32, 44.32, 44.27, 25.44.

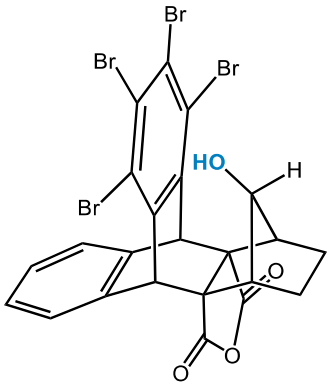

1,2,3,4-tetrabromo-15-hydroxy-9,10-dihydro-9,10-[4,7]methanoisobenzofuranoanthracene-12,14-dione (19). Compound **11** (0.02 g, 0.056 mmol) was dissolved with 20 mL DCM in a 100-mL round-bottom flask, then Br_2 (0.045 mL, 0.78 mmol) and elemental iron (15 mg, 0.26 mmol, cat.) were added. The reaction was stirred at room temperature for 24 h, and monitored by NMR until formation of the tetrabromo-product. The mixture was concentrated under reduced pressure and purified by silica gel chromatography with a 30% ethyl acetate and hexanes solution. Product **19** was isolated as white crystal (0.015 g, 0.022 mmol, 40.0% yield). ^{1}H NMR ($CDCl_3$) δ 7.31-7.34 (m, 2H), 7.19-7.21 (m, 2H), 5.36 (s, 2H), 4.06 (d, 1H, J = 2.85 Hz), 2.55 (m, 2H), 1.79-1.85 (m, 2H), 1.36-1.42 (m, 2H), 0.97 (d, 1H, J = 3.88 Hz); ^{13}C NMR ($CDCl_3$) δ 172.52, 144.18, 139.70, 128.38, 126.44, 126.05, 123.46, 83.84, 68.01, 50.90, 46.33, 25.07.

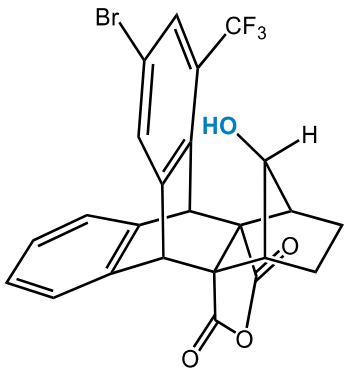

2-bromo-15-hydroxy-4-(trifluoromethyl)-9,10-dihydro-9,10-[4,7]methanoisobenzofuranoanthracene -12,14-dione (20). Compound **16** (0.025 g, 0.059 mmol) was dissolved in 20 mL DCM in a 100-mL round-bottom flask, then Br_2 (0.03 mL, 0.6 mmol) and elemental iron (15 mg, 0.26 mmol, cat.) were added. The reaction was allowed to stir at room temperature for 10 h. The mixture was concentrated under reduced pressure and then purified by silica gel chromatography with a 30% ethyl acetate and hexanes solution (0.017 g, 0.034 mmol, 57% yield). ^{1}H NMR ($CDCl_3$) δ 7.56 (d, 1H, *J* =1.50 Hz), 7.50 (d, 1H, *J* =1.66 Hz), 7.31-7.23 (m, 2H), 7.21-7.14 (m, 2H), 5.16 (s, 1H), 4.73 (s, 1H), 4.01 (s, 1H), 2.54 (s, 2H), 1.84-1.78 (m, 2H), 1.42-1.36 (m, 2H), 0.64 (d, 1H, *J* =3.76 Hz); ^{13}C NMR ($CDCl_3$) δ 172.97, 172.75, 146.60, 140.43, 140.31, 139.94, 131.36, 128.23, 128.20, 126.12 (q, *J* =5.13 Hz), 126.03, 125.74, 119.63, 83.97, 67.97, 67.92, 48.87, 46.48, 46.26, 45.46, 25.18, 25.05; ^{19}F NMR ($CDCl_3$) δ -59.98 (s, 1F); HRMS (ESI-) calc for $C_{24}H_{15}F_3O_4Br$-: 503.0111, found 503.0111.

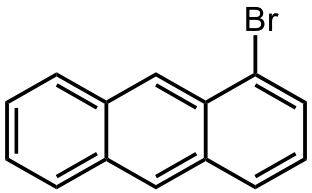

1-Bromoanthracene (21). Synthesized by following the synthetic route found in the literature.[8] Spectral and analytical data were in agreement with previous reports.[9]

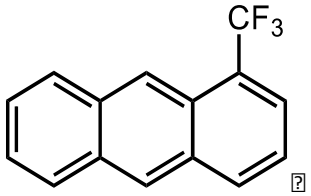

1-Trifluoromethylanthracene[10] **(22).** To a flame dried round-bottom flask were added **21** (1.1 g, 4.28 mmol), Sodium trifluoroacetate (5.5 g, 40.44 mmol), CuI (1.8 g, 9.45 mmol). To the mixture was added N-methyl-2-pyrrolidone 20 mL. The mixture was heated to 160 °C under N_2 and stirred for 14 h. The solvent was distilled off under reduced pressure, and 20 mL water was added to the crude product, which was extracted with ethyl acetate (4 x 20 mL). The organic fractions were combined, dried with $MgSO_4$ and concentrated under reduced pressure. The crude product was purified by silica gel chromatography with pure hexane to give **22** (0.8 g 3.25 mmol, 75.9% yield). ^{1}H NMR ($CDCl_3$) δ 8.76 (s, 1H), 8.48 (s, 1H), 8.16 (d, 1H, J = 8.6), 8.10-8.05 (m. 1H), 8.04-7.98 (m, 1H), 7.88 (d, 1H, J = 7.0), 7.58-7.51 (m, 2H), 7.45 (t, 1H, J = 7.8); ^{13}C NMR ($CDCl_3$) δ 133.34, 132.45, 131.79, 131.75, 128.91, 127.98, 127.54, 126.52, 126.49, 126.43, 125.02 (q, J = 6.0 Hz), 123.62 (q,

[8] Michio, G.; Kazushi, S.; Shinya, S.; Shinji, T. *Synthesis* **2005**, *13,* 2116-2118.
[9] Netka, J.; Crump, S. L.; Rickborn, B. *J. Org. Chem.* **1986**, *51*, 1189-1199.
[10] Carr, G. E.; Chambers, R. D.; Holmes, T. F. *J. Chem. Soc., Perkin Trans. 1* **1988**, *1,* 921-926.

J = 2.3 Hz), 123.19; ^{19}F NMR ($CDCl_3$) δ -60.67 (s, 1F); HRMS (ESI-) calc for $C_{15}H_8F_3$-: 245.0584 found 245.0584.

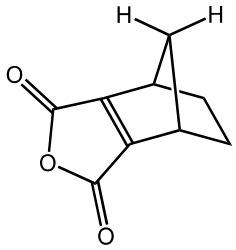

4,5,6,7-tetrahydro-4,7-methanoisobenzofuran-1,3-dione (23). Synthesized by following the synthetic route found in the literature.[11] Spectral and analytical data were in agreement with previous reports.

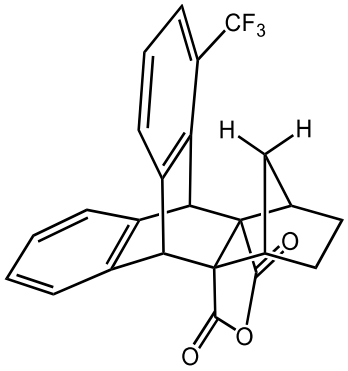

4-(trifluoromethyl)-9,10-dihydro-9,10-[4,7]methanoisobenzo-furanoanthracene-12,14-dione (24). In a sealed glass pressure vessel were combined **23** (0.22 g, 1.34 mmol), **12** (0.30 g, 1.22 mmol) and 1,2-dichlorobenzene (2 mL). The vessel was then sealed and heated at 180 °C for 14 h. The crude product was purified by silica gel column chromatography with 15% ethyl acetate and hexanes solution to give product **24** (0.21 g,

[11] Diels, O.; Alder, K. *Liebigs Ann. Chem.* **1931**, *490*, 236−242.

0.61 mmol, 50% yield). ^{1}H NMR ($CDCl_3$) δ 7.51 (t, 2H, *J* = 7.03 Hz), 7.35-7.27 (m, 3H), 7.22-7.17 (m, 2H), 5.17 (s, 1H), 4.74 (s, 1H), 2.65 (s, 1H), 2.56 (s, 1H), 1.64-1.58 (m, 2H), 1.45-1.39 (m, 2H), 0.89 (d, 1H, *J* = 11.42 Hz), 0.05-(-0.01) (m, 1H); ^{13}C NMR ($CDCl_3$) δ 173.10, 172.81, 142.52, 139.67, 139.10 (q, *J* = 1.96 Hz), 138.99, 128.66, 128.09, 127.36, 125.78, 125.48, 125.42, 124.11 (q, *J* = 6.03 Hz), 66.03, 65.76, 49.24, 45.77 (q, *J* = 1.83 Hz), 43.26, 42.69, 38.81, 27.54; ^{19}F NMR ($CDCl_3$) δ -59.25 (s, 1F); HRMS (ESI+) calc for $C_{24}H_{17}F_3O_3Na^+$: 433.1022, found 433.1026.

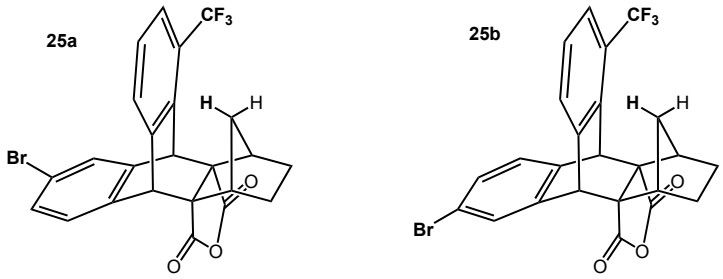

3-bromo-5-(trifluoromethyl)-9,10-dihydro-9,10-[4,7]methanoisobenzofuranoanthracene-12,14-dione and **2-bromo-5-(trifluoromethyl)-9,10-dihydro-9,10-[4,7]methanoisobenzofuranoanthracene-12,14-dione (25a and 25b).** Compound **24** (0.05 g, 0.12 mmol) was dissolved with 15 mL DCM in a 100 mL round-bottom flask, then Br_2 (0.012 mL, 0.24 mmol) and elemental iron (15 mg, 0.26 mmol, cat.) were added. The reaction was heated to reflux for 10 h. The mixture was concentrated under reduced pressure and then purified by prep. HPLC with a 15% ethyl acetate and hexanes solution. Product **25 (1)** (0.012 g, 0.025 mmol, 21% yield) and **25 (2)** (0.012 g, 0.025 mmol, 21% yield) were isolated. We were unable to definitively assign which isomer is which by the characterization techniques that were used, but we are

confident that the above are the two isomers that formed.

25 (1): ^{1}H NMR ($CDCl_3$) δ 7.56-7.46 (m, 2H), 7.36-7.31 (m, 2H), 7.17 (d, 1H, *J* = 8.01 Hz), 5.12 (s, 1H), 4.71 (s, 1H), 2.64 (s, 1H), 2.56 (s, 1H), 1.59-1.65 (m, 2H), 1.46-1.38 (m, 2H), 0.89 (d, 1H, *J* = 11.45 Hz), 0.02-(-0.05) (m, 1H); ^{13}C NMR ($CDCl_3$) δ 172.84, 172.47, 142.08, 141.12, 138.72, 131.16, 128.82, 128.71, 127.69, 126.84, 124.35 (d, *J* = 5.19 Hz), 121.90, 65.70, 65.50, 48.74, 43.30, 42.75, 38.81, 27.50.

25 (2): ^{1}H NMR ($CDCl_3$) δ 7.56-7.47 (m, 1H), 7.45 (d, 1H, *J* = 1.82 Hz), 7.36-7.31 (m, 2H), 7.19 (d, 1H, *J* = 7.92 Hz), 5.13 (s, 1H), 4.70 (s, 1H), 2.65 (s, 1H), 2.57 (s, 1H), 1.59-1.66 (m, 2H), 1.45-1.39 (m, 2H), 0.90 (d, 1H, *J* = 11.89 Hz), 0.02-(-0.04) (m, 1H); ^{13}C NMR ($CDCl_3$) δ 172.74, 172.57, 141.79, 138.66, 138.05, 131.14, 128.80, 128.55, 127.64, 127.18, 124.40 (q, *J* = 4.70 Hz), 121.92, 65.76, 65.42, 48.94, 45.29, 43.32, 42.73, 38.82, 27.51.

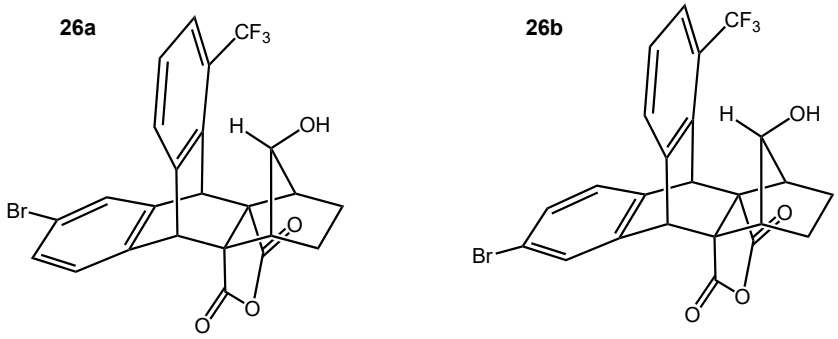

3-bromo-15-hydroxy-5-(trifluoromethyl)-9,10-dihydro-9,10-[4,7]methanoisobenzofuranoanthracene -12,14-dione (16a) and 2-bromo-15-hydroxy-5-(trifluoromethyl)-9,10-dihydro-9,10-[4,7]methano isobenzofuranoanthracene-12,14-dione (26b). To a 100 mL round bottom flask was added a mixture of **15** and **15-down** (0.050 g, 0.12 mmol, **15**:**15-down** = 2.5:1). Elemental iron (0.036 g, 0.64 mmol), Br_2 (0.43 g, 2.69 mmol), and CH_2Cl_2 (20 mL) were added. The solution was heated to reflux for 5 hours, and monitored by NMR. The mixture was concentrated under reduced pressure and purified by silica gel column chromatography with 15% ethyl acetate and hexanes solution. Then the mixture was further purified by prep. HPLC. Starting material **15** (0.008 g, 0.019 mmol) was collected, as were products **26 (1)** (0.008 g, 0.016 mmol, 13.3% yield), **26 (2)** (0.007 g, 0.014 mmol, 11.7% yield), **31 (1)** (0.005 g, 0.010 mmol, 8.33% yield), and **31 (2)** (0.004 g. 0.008 mmol, 6.67% yield).

26 (1): ^{1}H NMR ($CDCl_3$) δ 7.58-7.52 (m, 2H), 7.44 (d, 1H, J = 1.80), 7.36 (t, 1H, J = 7.79), 7.34 (dd, 1H, J^1 = 7.94, J^2 = 1.95), 7.18 (d, 1H, J = 7.99), 5.13 (s, 1H), 4.70 (s, 1H), 2.53-2.43 (m, 3H), 2.09-2.03 (m, 2H), 1.40-1.35 (m, 2H), 1.14 (d, 1H, J =3.93); ^{13}C NMR ($CDCl_3$) δ 171.99, 171.84, 142.58, 141.42, 139.39, 137.67, 131.32, 128.79, 128.64, 127.82,

127.25, 124.52 (d, J = 5.33), 122.10, 63.34, 63.10, 48.78, 46.65, 46.17, 45.20, 24.11, 24.06; HRMS (ESI+) calc for $C_{24}H_{16}BrF_3O_4Na^+$: 527.007627, found 527.007300.

26 (2): ^{1}H NMR ($CDCl_3$) δ 7.58-7.52 (m, 2H), 7.46 (s, 1H, J = 1.94), 7.36 (t, 1H, J = 7.54), 7.34 (dd, 1H, J^1 = 7.85, J^2 = 1.93), 7.16 (d, 1H, J = 7.84), 5.11 (s, 1H), 4.72 (s, 1H), 2.53-2.43 (m, 3H), 2.09-2.03 (m, 2H), 1.40-1.35 (m, 2H), 1.14 (d, 1H, J =3.03); ^{13}C NMR ($CDCl_3$) δ 172.09, 171.74, 142.86, 140.74, 139.09, 138.35, 131.35, 128.90, 128.69, 127.86, 126.92, 124.48 (d, J = 5.16), 122.08, 63.31, 63.15, 48.59, 46.62, 46.19, 45.40, 24.12, 24.06; HRMS (ESI+) calc for $C_{24}H_{16}BrF_3O_4Na^+$: 527.007627, found 527.007449.

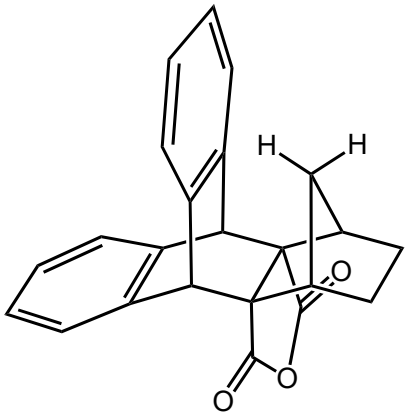

9,10-Dihydro-9,10-[4,7]methanoisobenzofuranoanthracene-12,14-dione (27). In a flame-dried 50-mL round bottom flask were combined **23** (1.00 g, 6.09 mmol), anthracene (1.00 g, 5.61 mmol) and toluene (20 mL). The combined solution was heated to reflux overnight. The mixture was concentrated under reduced pressure and then purified by silica gel column chromatography with a 10% ethyl acetate and hexanes solution. Product **27** (1.36 g, 3.97 mmol, 70.8% yield) was collected. Spectral and analytical data were in

agreement with previous reports.[12]

[12] Holl, M. G.; Struble, M. D.; Singal, P.; Siegler, M. A.; Lectka, T. *Angew. Chem. Int. Ed.* **2016,** *55,* 8266-8269.

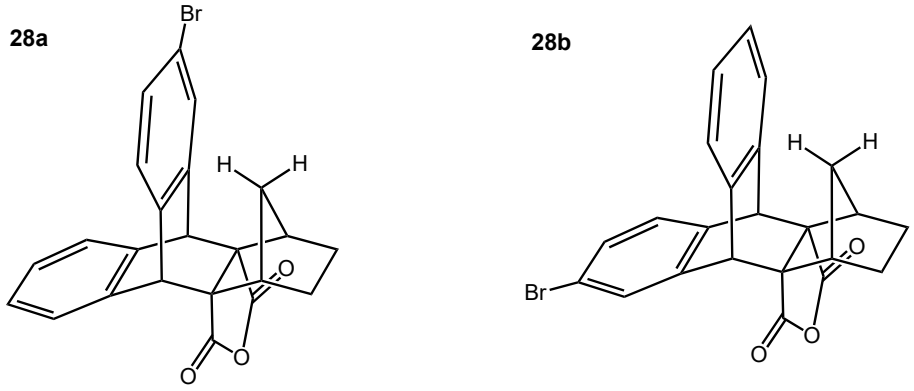

3-Bromo-9,10-dihydro-9,10-[4,7]methanoisobenzofuranoanthracene-12,14-dione (28a). In a sealed glass pressure vessel with stir bar were combined **27** (0.12 g, 0.35 mmol), Br_2 (0.62 g, 3.87 mmol) and CH_3CN (5 mL). The vessel was then sealed and heated to 140 °C for 12 h with stirring. The Crude product was purified by silica gel column chromatography with 15% ethyl acetate and hexanes solution. Then the mixture was further purified by prep. HPLC. **28a** (0.080g, 0.19 mmol, 54.3% yield) and **28b** (0.011 g, 0.03 mmol, 8.6% yield) were collected. ^{1}H NMR ($CDCl_3$) δ 7.48 (d, 1H, J = 1.95), 7.35 (dd, 1H, J^1 = 7.88, J^2 = 1.95), 7.30-7.25 (m, 2H), 7.23-7.13 (m, 3H), 4.64 (s, 1H), 4.62 (s, 1H), 2.58-2.51 (m, 2H), 1.64-1.57 (m, 2H), 1.44-1.37 (m, 2H), 0.91 (d, 1H, J = 11.60), 0.23-0.15 (m, 1H); HRMS (ESI-) calc for $C_{23}H_{17}BrO_3K^+$: 458.999265, found 458.999015.

2-Bromo-9,10-dihydro-9,10-[4,7]methanoisobenzofuranoanthracene-12,14-dione (28b). Isolated with **31**. ^{1}H NMR ($CDCl_3$) δ 7.44 (d, 1H, J = 2.11), 7.32-7.28 (m, 3H), 7.23-7.20 (m, 2H), 7.15 (d, 1H, J = 7.95), 4.63 (s, 1H), 4.62 (s, 1H), 2.52 (s, 2H), 1.63-1.57 (m, 2H), 1.44-1.37 (m, 2H), 0.84 (d, 1H, J = 11.44), 0.04-(-0.02) (m, 1H); HRMS (ESI-) calc for $C_{23}H_{17}BrO_3Na^+$: 443.025328, found 443.025568.

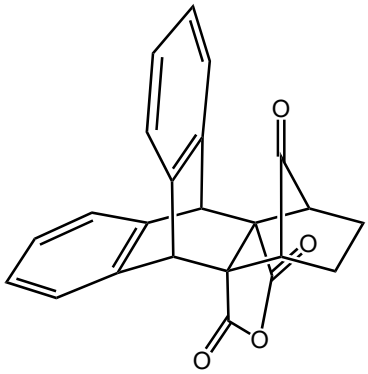

9,10-dihydro-9,10-[4,7]methanoisobenzofuranoanthracene-12,14,15-trione (29). To a 100 mL round-bottom flask equipped with a condenser were added **14** (0.32 g, 0.89 mmol), crushed 4 Å molecular sieves (2.60 g), and potassium carbonate (1.20 g). The mixture was suspended in DCM (20 mL) followed by addition of PCC (0.32 g, 1.48 mmol). The solution was refluxed for 2 h. The mixture was concentrated under reduced pressure and then purified by silica gel column chromatography with 15% ethyl acetate and hexanes solution. **29** (0.29 g, 0.81 mmol, 91% yield) was collected as white crystals. ^{1}H NMR ($CDCl_3$) δ 7.38-7.33 (m, 4H), 7.29-7.26 (m, 2H), 7.26-7.22 (m, 2H), 4.70 (s, 2H), 2.37-2.34 (m, 2H), 1.87-1.81 (m, 2H), 1.61-1.56 (m, 2H); ^{13}C NMR ($CDCl_3$) δ 200.51, 171.33, 138.19, 128.52, 128.25, 126.58, 125.52, 61.03, 49.11, 46.71, 19.72; HRMS (ESI+) calc for $C_{23}H_{16}O_4Na^+$: 379.094080, found 379.093961.

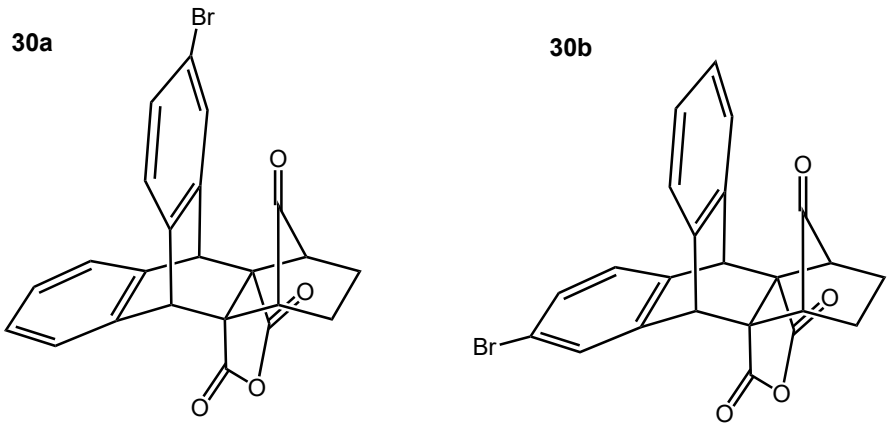

3-bromo-9,10-dihydro-9,10-[4,7]methanoisobenzofuranoanthracene-12,14,15-trione (30a). To a 100 mL round bottom flask was added **29** (0.10 g, 0.28 mmol). Fe metal (0.036 g, 0.64 mmol), Br_2 (0.64 g, 4.00 mmol), and CH_2Cl_2 (20 mL). The solution was heated to reflux for 2 hours. The mixture was concentrated under reduced pressure and purified by silica gel column chromatography with 15% ethyl acetate and hexanes solution. **29** (0.063 g, 0.175 mmol, 62.5% recycled), **30a** (0.023 g, 0.053 mmol, 18.9% yield), and **30b** (0.026 g, 0.059 mmol, 21.3% yield) were collected. ^{1}H NMR ($CDCl_3$) δ 7.51 (d, 1H, J=1.93 Hz), 7.41 (dd, 1H, J^1=8.08 Hz, J^2=1.91 Hz), 7.37-7.31 (m, 2H), 7.28-7.24 (m, 2H), 7.21 (d, 1H, J=7.98 Hz), 4.68 (s, 1H), 4.66 (s, 1H), 2.40-2.34 (m, 2H), 1.91-1.83 (m, 2H), 1.64-1.55 (m, 2H); ^{13}C NMR ($CDCl_3$) δ 200.69, 171.02, 170.99, 139.82, 137.80, 137.50, 136.63, 131.50, 129.66, 128.52, 128.50, 127.95, 125.65, 125.58, 122.33, 60.68, 60.66, 48.82, 48.66, 46.71, 46.60, 19.73; HRMS (ESI+) calc for $C_{23}H_{15}BrO_4Na^+$: 457.004593, found 457.004632.

2-bromo-9,10-dihydro-9,10-[4,7]methanoisobenzofuranoanthracene-12,14,15-trione (30b). Isolated with **30a**. ^{1}H NMR ($CDCl_3$) δ 7.50 (d, 1H, J=1.93 Hz), 7.38 (dd, 1H, J^1

=7.97 Hz, J^2=1.96 Hz), 7.36-7.32 (m, 2H), 7.30-7.26 (m, 2H), 7.22 (d, 1H, J =7.98 Hz), 4.67 (s, 1H), 4.65 (s, 1H), 2.37-2.33 (m, 2H), 1.89-1.82 (m, 2H), 1.63-1.56 (m, 2H); ^{13}C NMR ($CDCl_3$) δ 200.17, 171.10, 171.02, 140.37, 137.28, 137.21, 136.95, 131.29, 128.81, 128.79, 128.66, 126.98, 126.71, 126.65, 122.06, 60.74, 60.72, 48.79, 48.61, 46.65, 19.71; HRMS (ESI+) calc for $C_{23}H_{15}BrO_4Na^+$: 457.004593, found 457.004603.

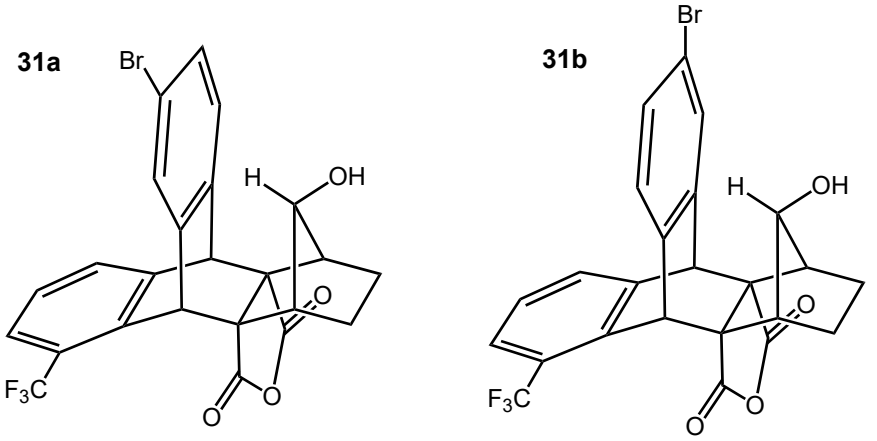

6-bromo-15-hydroxy-1-(trifluoromethyl)-9,10-dihydro-9,10-[4,7]methanoisobenzofuranoanthracene -12,14-dione (31a) and **7-bromo-15-hydroxy-1-(trifluoromethyl)-9,10-dihydro-9,10-[4,7]methano isobenzofuranoanthracene-12,14-dione (31b).** Isolated with **26a** and **26b.**

31 (1): ^{1}H NMR ($CDCl_3$) δ 7.52 (d, 1H, J = 1.78), 7.47 (t, 2H, J = 8.07), 7.41 (dd, 1H, J^1 = 7.67, J^2 = 1.90), 7.32-7.26 (m, 2H), 5.14 (s, 1H), 4.69 (s, 1H), 2.74 (s, 1H), 2.47 (s, 2H), 2.11-2.06 (m, 2H), 1.40-1.36 (m, 2H), 1.25 (d, 1H, J =4.39); ^{13}C NMR ($CDCl_3$) δ 172.15, 170.64, 142.68, 141.19, 138.99, 138.26, 131.02, 129.10, 128.49, 127.82, 126.81, 124.87, 121.64, 63.02, 62.35, 48.44, 46.67, 46.39, 45.39, 23.94; HRMS (ESI+) calc for $C_{24}H_{16}BrF_3O_4Na^+$: 527.007627, found 527.007281.

31 (2): ^{1}H NMR ($CDCl_3$) δ 7.54 (d, 1H, J = 1.87), 7.50-7.43 (m, 2H), 7.40 (dd, 1H, J^1 = 7.83, J^2 = 1.89), 7.31-7.22 (m, 2H), 5.12 (s, 1H), 4.71 (s, 1H), 2.72 (s, 1H), 2.49-2.41 (m, 2H), 2.12-2.05 (m, 2H), 1.42-1.35 (m, 2H), 1.25 (d, 1H, J =3.98); ^{13}C NMR ($CDCl_3$) δ 172.19, 170.60, 142.11, 141.47, 139.54, 137.98, 130.98, 129.01, 128.60, 127.86, 126.63,

124.86, 121.70, 62.98, 62.41, 48.31, 46.69, 46.37, 45.51, 23.96, 24.90; HRMS (ESI+) calc for $C_{24}H_{16}BrF_3O_4Na^+$: 527.007627, found 527.007675.

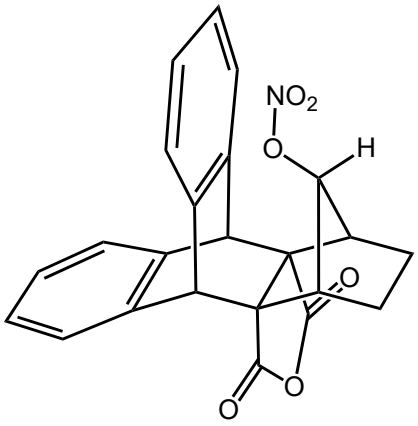

12,14-dioxo-9,10-dihydro-9,10-[4,7]methanoisobenzofuranoanthracen-15-yl nitrate (32). In a 25-mL round bottom flask was added **11** (0.050 g, 0.14 mmol), NH_4NO_3 (0.009 g, 0.11 mmol), trifluoroacetic anhydride (cat.) and CH_3CN (5 mL). The reaction was allowed to stir overnight at room temperature. The mixture was concentrated under reduced pressure and purified by silica gel column chromatography with 15% ethyl acetate and hexanes solution. **32** (0.022 g, 0.054 mmol, 38.6% yield) and **11** (0.027 g, 0.075 mmol, 53.6% recycled) were collected. ^{1}H NMR ($CDCl_3$) δ 7.32-7.28 (m, 2H), 7.26-7.22 (m, 2H), 7.19-7.15 (m, 2H), 7.14-7.11 (m, 2H), 4.69 (s, 2H), 4.59 (s, 1H), 2.90 (m, 2H), 1.98-1.93 (m, 2H), 1.61-1.56 (m, 2H); ^{13}C NMR ($CDCl_3$) δ 172.56, 141.11, 139.91, 128.18, 127.72, 125.54, 125.22, 90.49, 68.06, 48.94, 43.82, 25.08; HRMS (ESI+) calc for $C_{23}H_{17}NO_6Na^+$: 426.094808, found 426.094763.

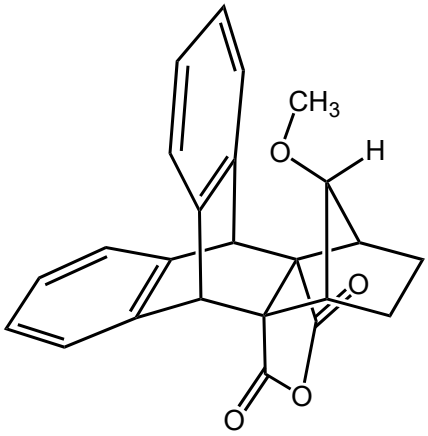

15-methoxy-9,10-dihydro-9,10-[4,7]methanoisobenzofuranoanthracene-12,14-dione (33). To a 10-mL round bottom flask was added **11** (0.020 g, 0.056 mmol), NaH (0.013 g, 0.54 mmol) and DMSO (3 mL), then add CH_3I (0.08 g, 0.56 mmol). The mixture was allowed to stir at room temperature for 1 hour, then quenched by 3 mL of water. Then the mixture was transferred into a separatory funnel containing 20 mL water, and extracted with ethyl acetate (3 x 20 mL). The organic fractions were combined, dried with $MgSO_4$ and concentrated under reduced pressure. The crude product was purified by silica gel chromatography with 20% ethyl acetate and hexanes to give **33** (0.016 g, 0.043 mmol, 76.7% yield). ^1H NMR ($CDCl_3$) δ 7.31-7.26 (m, 2H), 7.25-7.21 (m, 2H), 7.16-7.06 (m, 4H), 4.67 (s, 2H), 3.36 (s, 1H), 2.66-2.63 (m, 2H), 2.50 (s, 3H), 1.81-1.73 (m, 2H), 1.45-1.37 (m, 2H); ^{13}C NMR ($CDCl_3$) δ 173.76, 141.81, 141.69, 127.35, 126.42, 125.39, 124.46, 93.18, 68.14, 59.55, 49.25, 43.12, 25.03; HRMS (ESI+) calc for $C_{24}H_{20}O_4Na^+$: 395.125380, found 395.125533.

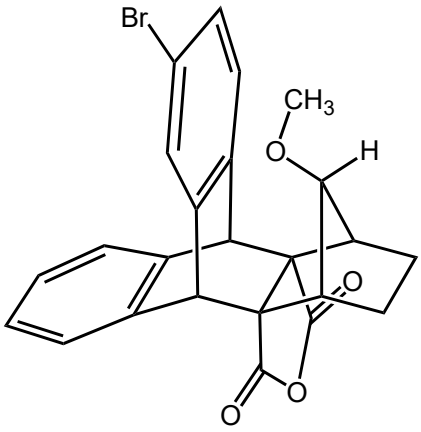

2-bromo-15-methoxy-9,10-dihydro-9,10-[4,7]methanoisobenzofuranoanthracene-12,14-dione (34). To a 10-mL round bottom flask was added **33** (0.006 g, 0.016 mmol). Br_2 (0.62 g, 3.87 mmol), and CH_2Cl_2 (3 mL) The solution was stirred at room temperature for 15 min, then quenched with 3 mL acetone. The mixture was concentrated under reduced pressure and purified by silica gel column chromatography with 20% ethyl acetate and hexanes solution to give **34** (0.005 g, 0.011 mmol, 69.2% yield). ^{1}H NMR ($CDCl_3$) δ 7.42 (d, 1H, *J* =1.92), 7.24-7.19 (m, 3H), 7.16-7.10 (m, 3H), 4.64 (s, 1H), 4.61 (s, 1H), 3.38 (s, 1H), 2.66-2.60 (m, 2H), 2.58 (s, 3H), 1.82-1.74 (m, 2H), 1.44-1.37 (m. 2H); ^{13}C NMR ($CDCl_3$) δ 173.44, 173.36, 143.95, 141.25, 140.99, 140.89, 129.20, 127.72, 127.67, 127.55, 126.02, 125.60, 125.50, 119.92, 93.24, 68.01, 68.00, 59.30, 48.89, 48.80, 43.58, 42.86, 25.03, 25.00; HRMS (ESI+) calc for $C_{24}H_{19}BrO_4Na^+$: 473.035893, found 473.036223.

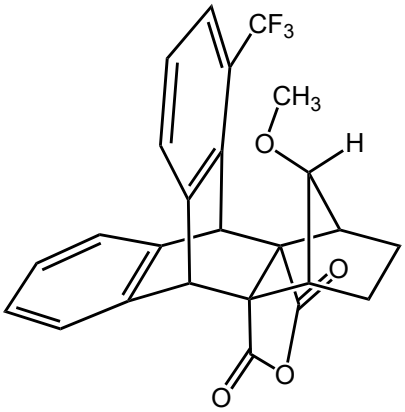

2-bromo-15-methoxy-4-(trifluoromethyl)-9,10-dihydro-9,10-[4,7]methanoisobenzofurano anthracene-12,14-dione (35). To a 10-mL round bottom flask was added **16** (0.056 g, 0.13 mmol), NaH (0.013 g, 0.54 mmol) and DMSO (3 mL), then add CH_3I (0.08 g, 0.56 mmol). The mixture was stirred at room temperature for 1 hour, and quenched with 3 mL of water. Then the mixture was transferred into a separate funnel containing 20 mL water, and extracted with ethyl acetate (3 x 20 mL). The organic fractions were combined, dried with $MgSO_4$ and concentrated under reduced pressure. The crude product was purified by silica gel chromatography with 20% ethyl acetate and hexanes to give **35** (0.042 g, 0.10 mmol, 73.4% yield). ^{1}H NMR ($CDCl_3$) δ 7.43 (d, 1H, *J* =7.46), 7.37 (d, 1H, *J* =7.95), 7.30-7.22 (m, 2H), 7.19-7.11 (m, 3H), 5.16 (s, 1H), 4.73 (s, 1H), 2.69 (s, 1H), 2.61 (s, 1H), 2.49 (s, 3H), 1.82-1.74 (m, 2H), 1.45-1.35 (m, 2H); ^{13}C NMR ($CDCl_3$) δ 173.44, 173.19, 143.89, 141.30, 140.59 (q, *J* =2.13), 140.55, 127.94, 127.84, 127.82, 126.03, 125.88, 125.49, 123.03 (q, *J* =5.06), 93.26, 67.72, 67.70, 59.59, 49.11, 45.73, 45.71, 43.60, 42.78, 24.98, 24.95; HRMS (ESI+) calc for $C_{25}H_{19}F_3O_4Na^+$: 463.112765, found 463.112499.

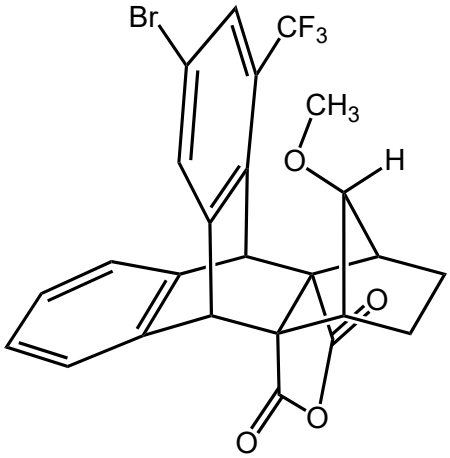

15-methoxy-4-(trifluoromethyl)-9,10-dihydro-9,10-[4,7]methanoisobenzofuranoanthracene-12,14-dione (36). To a 10 mL round bottom flask was added **35** (0.020 g, 0.045 mmol) and Br_2 (0.62 g, 3.87 mmol), The mixture was stir at room temperature for 45 min, then quenched by 3 mL acetone. The mixture was concentrated under reduced pressure and purified by silica gel column chromatography with 20% ethyl acetate and hexanes solution to give **36** (0.010 g, 0.019 mmol, 42% yield) and **35** (0.009 g, 0.020 mmol, 44% recycled). ^{1}H NMR ($CDCl_3$) δ 7.57 (d, 1H, *J* =1.76), 7.51 (d, 1H, *J* =1.76), 7.29-7.22 (m, 2H), 7.18-7.13 (m, 2H), 5.12 (s, 1H), 4.68 (s, 1H), 3.36 (s, 1H), 2.67-2.60 (m, 2H), 2.58 (s, 3H), 1.84-1.75 (m, 2H), 1.46-1.36 (m, 2H); ^{13}C NMR ($CDCl_3$) δ 173.02, 172.86, 146.10, 140.48, 139.93, 139.80, 130.81, 128.15, 128.12, 125.96, 125.89 (q, *J* =4.97), 125.67, 119.45, 93.29, 67.58, 67.54, 59.45, 48.76, 45.44, 43.29, 43.20, 24.95, 24.88; HRMS (ESI+) calc for $C_{24}H_{16}BrF_3O_4Na^+$: 541.023277, found 541.022976.

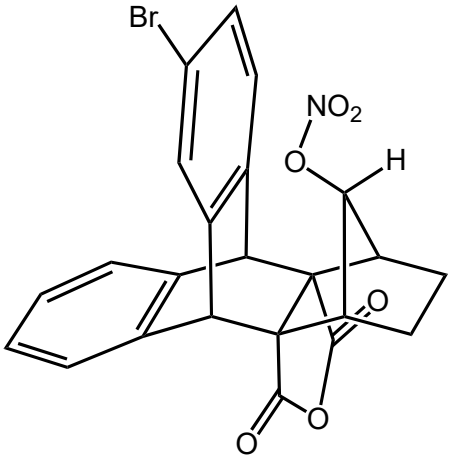

3-bromo-12,14-dioxo-9,10-dihydro-9,10-[4,7]methanoisobenzofuranoanthracen-15-yl nitrate (37). In a 25-ml round bottom flask was added **17** (15 mg, 0.034 mmol), NH_4NO_3 (3 mg, 0.038 mmol), Trifluoroacetic anhydride (cat.) and CH_3CN (5 mL). The reaction was allowed to stir 1 hour at room temperature. The mixture was concentrated under reduced pressure and purified by silica gel column chromatography with 20% ethyl acetate and hexanes solution. **37** (14 mg, 0.029 mmol, 85.3% yield) were collected. ^{1}H NMR ($CDCl_3$) δ 7.44 (d, 1H, *J*=1.96Hz), 7.31 (dd, 1H, J^1=7.96Hz, J^2=1.94Hz), 7.25-7.22 (m, 2H), 7.19-7.13 (m, 3H), 4.68 (s, 2H), 4.64 (s, 1H), 2.88 (m, 2H), 2.02-1.94 (m, 2H), 1.62-1.54 (m, 2H); ^{13}C NMR ($CDCl_3$) δ 172.24, 172.16, 142.11, 140.57, 140.31, 139.00, 131.09, 128.34, 128.02, 127.99, 126.62, 125.72, 125.60, 121.93, 90.14, 67.86, 67.80, 48.50, 48.43, 43.80, 25.08, 25.04;

Reference:

(1) Lewis, G. N. THE ATOM AND THE MOLECULE. *J. Am. Chem. Soc.* **1916**, *38* (4), 762–785.

(2) Pauling, L. The Nature of the Chemical Bond. Application of Results Obtained from the Quantum Mechanics and from a Theory of Paramagnetic Susceptibility to the Structure of Molecules. *J. Am. Chem. Soc.* **1931**, *53* (4), 1367–1400.

(3) Lennard-Jones, J. E. The Electronic Structure of Some Diatomic Molecules. *Trans. Faraday Soc.* **1929**, *25* (0), 668.

(4) Politzer, P.; Murray, J. S.; Concha, M. C. Halogen Bonding and the Design of New Materials: Organic Bromides, Chlorides and Perhaps Even Fluorides as Donors. *J. Mol. Model.* **2007**, *13* (6–7), 643–650.

(5) Politzer, P.; Lane, P.; Concha, M. C.; Ma, Y.; Murray, J. S. An Overview of Halogen Bonding. *Journal of Molecular Modeling*. 2007, pp 305–311.

(6) Parisini, E.; Metrangolo, P.; Pilati, T.; Resnati, G.; Terraneo, G. Halogen Bonding in Halocarbon–protein Complexes: A Structural Survey. *Chem. Soc. Rev.* **2011**, *40* (5), 2267.

(7) Lu, Y.; Shi, T.; Wang, Y.; Yang, H.; Yan, X.; Luo, X.; Jiang, H.; Zhu, W. Halogen Bonding - A Novel Interaction for Rational Drug Design? *J. Med. Chem.* **2009**, *52* (9), 2854–2862.

(8) Domagała, M.; Matczak, P.; Palusiak, M. Halogen Bond, Hydrogen Bond and N...C Interaction - On Interrelation among These Three Non-covalent Interactions. *Comput. Theor. Chem.* **2012**, *998*, 26–33.

(9) Guan, L.; Mo, Y. Electron Transfer in Pnicogen Bonds. *J. Phys. Chem. A* **2014**, *118* (39), 8911–8921.

(10) Politzer, P.; Riley, K. E.; Bulat, F. A.; Murray, J. S. Perspectives on Halogen Bonding and Other σ-Hole Interactions: Lex Parsimoniae (Occam's Razor). *Comput. Theor. Chem.* **2012**, *998*, 2–8.

(11) Wang, C.; Guan, L.; Danovich, D.; Shaik, S.; Mo, Y. The Origins of the Directionality of Non-covalent Intermolecular Interactions[#]. *Journal of Computational Chemistry*. John Wiley and Sons Inc. 2015.

(12) Pauling, L. The Nature of the Chemical Bond. Application of Results Obtained from the Quantum Mechanics and from a Theory of Paramagnetic Susceptibility to the Structure of Molecules. *J. Am. Chem. Soc.* **1931**, *53* (4), 1367–1400.

(13) Arunan, E.; Desiraju, G. R.; Klein, R. A.; Sadlej, J.; Scheiner, S.; Alkorta, I.; Clary, D. C.; Crabtree, R. H.; Dannenberg, J. J.; Hobza, P.; et al. Definition of the Hydrogen Bond (IUPAC Recommendations 2011). *Pure Appl. Chem.* **2011**, *83* (8), 1637–1641.

(14) Struble, M. D.; Holl, M. G.; Coombs, G.; Siegler, M. A.; Lectka, T. Synthesis of a Tight Intramolecular OH···Olefin Interaction, Probed by IR, 1H NMR, and Quantum Chemistry. *J. Org. Chem.* **2015**, *80* (9), 4803–4807.

(15) Struble, M. D.; Strull, J.; Patel, K.; Siegler, M. a; Lectka, T. Modulating " Jousting " C − F---H − C Interactions with a Bit of Hydrogen Bonding. **2014**, 6–11.

(16) Mo, Y.; Wang, C.; Guan, L.; Braïda, B.; Hiberty, P. C.; Wu, W. On the Nature of Blueshifting Hydrogen Bonds. *Chem. - A Eur. J.* **2014**, *20* (27), 8444–8452.

(17) Desiraju, G. R.; Ho, P. S.; Kloo, L.; Legon, A. C.; Marquardt, R.; Metrangolo, P.; Politzer, P.; Resnati, G.; Rissanen, K. Definition of the Halogen Bond (IUPAC Recommendations 2013). *Pure Appl. Chem.* **2013**, *85* (8), 1711–1713.

(18) Remsen, I.; Norris, J. F. The Action of the Halogens on the Methylamines. *Am Chem J* **1896**, *18*, 90–95.

(19) Guthrie, F.; Ch, A. GUTHRIE ON THE IODIDE OF IODAMMONIUM. CI 1 H. *Chem. Soc. Qu. J.* **1863**, *34*, 239.

(20) Hassel, O. Structural Aspects of Interatomic Charge-Transfer Bonding. *Science (80-.).* **1970**, *170* (3957), 497–502.

(21) Riley, K. E.; Murray, J. S.; Fanfrlík, J.; Řezáč, J.; Solá, R. J.; Concha, M. C.; Ramos, F. M.; Politzer, P. Halogen Bond Tunability II: The Varying Roles of Electrostatic and Dispersion Contributions to Attraction in Halogen Bonds. *J. Mol. Model.* **2013**, *19* (11), 4651–4659.

(22) Riley, K. E.; Murray, J. S.; Fanfrlík, J.; Řezáč, J.; Solá, R. J.; Concha, M. C.; Ramos, F. M.; Politzer, P. Halogen Bond Tunability I: The Effects of Aromatic Fluorine Substitution on the Strengths of Halogen-Bonding Interactions Involving Chlorine, Bromine, and Iodine. *J. Mol. Model.* **2011**, *17* (12), 3309–3318.

(23) Forni, A. Experimental and Theoretical Study of the Br···N Halogen Bond in Complexes of 1,4-Dibromotetrafluorobenzene with Dipyridyl Derivatives. *J. Phys. Chem. A* **2009**, *113* (14), 3403–3412.

(24) Baumli, S.; Endicott, J. A.; Johnson, L. N. Halogen Bonds Form the Basis for Selective P-TEFb Inhibition by DRB. *Chem. Biol.* **2010**, *17* (9), 931–936.

(25) Mukherjee, A.; Tothadi, S.; Desiraju, G. R. Halogen Bonds in Crystal Engineering: Like Hydrogen Bonds yet Different. *Acc. Chem. Res.* **2014**, *47* (8), 2514–2524.

(26) Fang, Y.; Li, A. Y.; Ma, F. Y. A Comparative Study of the Chalcogen Bond, Halogen Bond and Hydrogen Bond S···O/Cl/H Formed between SHX and HOCl. *J. Mol. Model.* **2015**, *21* (3).

(27) Nziko, V. D. P. N.; Scheiner, S. Intramolecular S···O Chalcogen Bond as Stabilizing Factor in Geometry of Substituted Phenyl-SF3 Molecules. *J. Org. Chem.* **2015**, *80* (4), 2356–2363.

(28) Azofra, L. M.; Scheiner, S. Tetrel, Chalcogen, and CH..O Hydrogen Bonds in Complexes Pairing Carbonyl-Containing Molecules with 1, 2, and 3 Molecules of CO2. *J. Chem. Phys.* **2015**, *142* (3), 1–10.

(29) Grabowski, S. New Type of Halogen Bond: Multivalent Halogen Interacting with π- and σ-Electrons. *Molecules* **2017**, *22* (12), 2150.

(30) Scheiner, S. Halogen Bonds Formed between Substituted Imidazoliums and N Bases of Varying N-Hybridization. *Molecules* **2017**, *22* (10), 1634.

(31) Galland, N.; Montavon, G.; Le Questel, J.-Y.; Graton, J. Quantum Calculations of At-Mediated Halogen Bonds: On the Influence of Relativistic Effects. *New J. Chem.* **2018**.

(32) Del Bene, J.; Alkorta, I.; Elguero, J. Halogen Bonding Involving CO and CS with Carbon as the Electron Donor. *Molecules* **2017**, *22* (11), 1955.

(33) Ibrahim, M. A. A.; Hasb, A. A. M.; Mekhemer, G. A. H. Role and Nature of Halogen Bonding in Inhibitor···receptor Complexes for Drug Discovery: Casein Kinase-2 (CK2) Inhibition as a Case Study. *Theor. Chem. Acc.* **2018**, *137* (3), 38.

(34) Wang, J.; Sánchez-Roselló, M.; Aceña, J. L.; Del Pozo, C.; Sorochinsky, A. E.; Fustero, S.; Soloshonok, V. A.; Liu, H. Fluorine in Pharmaceutical Industry: Fluorine-Containing Drugs Introduced to the Market in the Last Decade (2001-2011). *Chem. Rev.* **2014**, *114* (4), 2432–2506.

(35) Pan, Z.; Fan, Z.; Lu, B.; Cheng, J. Halogen-Bond-Promoted α-C−H Amination of Ethers for the Synthesis of Hemiaminal Ethers. *Adv. Synth. Catal.* **2018**.

(36) Heinen, F.; Engelage, E.; Dreger, A.; Weiss, R.; Huber, S. M. Iodine(III) Derivatives as Halogen Bonding Organocatalysts. *Angew. Chemie Int. Ed.* **2018**, *57* (14), 3830–3833.

(37) Chan, Y.-C.; Yeung, Y.-Y. Halogen Bond Catalyzed Bromocarbocyclization. *Angew. Chemie Int. Ed.* **2018**, *57* (13), 3483–3487.

(38) Nziko, V. D. P. N.; Scheiner, S. Catalysis of the Aza-Diels-Alder Reaction by Hydrogen and Halogen Bonds. *J. Org. Chem.* **2016**, *81* (6), 2589–2597.

(39) von der Heiden, D.; Bozkus, S.; Klussmann, M.; Breugst, M. Reaction Mechanism of Iodine-Catalyzed Michael Additions. *J. Org. Chem.* **2017**, *82* (8), 4037–4043.

(40) Jungbauer, S. H.; Huber, S. M. Cationic Multidentate Halogen-Bond Donors in Halide Abstraction Organocatalysis: Catalyst Optimization by Preorganization. *J. Am. Chem. Soc.* **2015**, *137* (37), 12110–12120.

(41) Li, J.; Hu, Y.-H.; Ge, C.-W.; Gong, H.-G.; Gao, X.-K. The Role of Halogen Bonding in Improving OFET Performance of a Naphthalenediimide Derivative. *Chinese Chem. Lett.* **2018**, *29* (3), 423–428.

(42) Carreras, L.; Serrano-Torné, M.; van Leeuwen, P. W. N. M.; Vidal-Ferran, A. XBphos-Rh: A Halogen-Bond Assembled Supramolecular Catalyst. *Chem. Sci.* **2018**.

(43) Sperati, C. A.; Starkweather, H. W. Fluorine-Containing Polymers. II. Polytetrafluoroethylene*. *Fortschritte Der Hochpolym.* **1961**, No. 2, 465–495.

(44) Rae, P. J.; Dattelbaum, D. M. The Properties of Poly(tetrafluoroethylene) (PTFE) in Compression. *Polymer (Guildf).* **2004**, *45* (22), 7615–7625.

(45) Ojima, I. Exploration of Fluorine Chemistry at the Multidisciplinary Interface of Chemistry and Biology. *Journal of Organic Chemistry*. 2013, pp 6358–6383.

(46) Biswas, S. K.; Vijayan, K. Friction and Wear of PTFE - a Review. *Wear* **1992**, *158* (1–2), 193–211.

(47) Wieleba, W. The Statistical Correlation of the Coefficient of Friction and Wear Rate of PTFE Composites with Steel Counterface Roughness and Hardness. *Wear* **2002**, *252* (9–10), 719–729.

(48) O'Hagan, D. Understanding Organofluorine Chemistry. An Introduction to the C–F Bond. *Chem. Soc. Rev.* **2008**, *37* (2), 308–319.

(49) Lemal, D. M. Perspective on Fluorocarbon Chemistry. *Journal of Organic Chemistry*. 2004, pp 1–11.

(50) Amii, H.; Uneyama, K. C-F Bond Activation in Organic Synthesis. *Chem. Rev.* **2009**, *109* (5), 2119–2183.

(51) Torrens, H. Carbon-Fluorine Bond Activation by Platinum Group Metal Complexes. *Coord. Chem. Rev.* **2005**, *249* (17–18 SPEC. ISS.), 1957–1985.

(52) Aizenberg, M.; Milstein, D. Catalytic Activation of Carbon-Fluorine Bonds by a Soluble Transition Metal Complex. *Science (80-.).* **1994**, *265* (5170), 359–361.

(53) Clot, E.; Eisenstein, O.; Jasim, N.; MacGregor, S. A.; McGrady, J. E.; Perutz, R. N. C-F and C-H

Bond Activation of Fluorobenzenes and Fluoropyridines at Transition Metal Centers: How Fluorine Tips the Scales. *Acc. Chem. Res.* **2011**, *44* (5), 333–348.

(54) Burdeniuc, J.; Jedicka, B.; Crabtree, R. H. Recent Advances in C–F Bond Activation. *Chem. Ber.* **1997**, *130* (2), 145–154.

(55) Kiplinger, J. L.; Richmond, T. G.; Osterberg, C. E. Activation of Carbon-Fluorine Bonds by Metal Complexes. *Chem. Rev.* **1994**, *94* (2), 373–431.

(56) Meier, G.; Braun, T. Catalytic C-F Activation and Hydrodefluorination of Fluoroalkyl Groups. *Angewandte Chemie - International Edition*. Wiley-Blackwell January 15, 2009, pp 1546–1548.

(57) Ferraris, D.; Cox, C.; Anand, R.; Lectka, T. C-F Bond Activation by Aryl Carbocations: Conclusive Intramolecular Fluoride Shifts between Carbon Atoms in Solution and the First Examples of Intermolecular Fluoride Ion Abstractions. *J. Am. Chem. Soc.* **1997**, *119* (18), 4319–4320.

(58) Nova, A.; Mas-Ballesté, R.; Lledós, A. Breaking C-F Bonds via Nucleophilic Attack of Coordinated Ligands: Transformations from C-F to C-X Bonds (X= H, N, O, S). *Organometallics*. American Chemical Society February 27, 2012, pp 1245–1256.

(59) Holl, M. G.; Struble, M. D.; Singal, P.; Siegler, M. A.; Lectka, T. Positioning a Carbon–Fluorine Bond over the π Cloud of an Aromatic Ring: A Different Type of Arene Activation. *Angew. Chemie - Int. Ed.* **2016**, *55* (29), 8266–8269.

(60) Martin, J. G.; Hill, R. K. Stereochemistry of the Diels-Alder Reaction. *Chem. Rev.* **1961**, *61* (6), 537–562.

(61) Eisch, J. J.; Hota, N. K.; Kozima, S. Synthesis of Pentaphenylborole, a Potentially Antiaromatic System. *Journal of the American Chemical Society*. American Chemical Society July 1969, pp 4575–4577.

(62) Braunschweig, H.; Kupfer, T. Recent Developments in the Chemistry of Antiaromatic Boroles. *Chem. Commun.* **2011**, *47* (39), 10903.

(63) Fagan, P. J.; Burns, E. G.; Calabrese, J. C. Synthesis of Boroles and Their Use in Low-Temperature Diels-Alder Reactions with Unactivated Alkenese. *J. Am. Chem. Soc.* **1988**, *110* (9), 2979–2981.

(64) Fagan, P. J.; Nugent, W. A.; Calabrese, J. C. Metallacycle Transfer from Zirconium to Main Group Elements: A Versatile Synthesis of Heterocycles. *J. Am. Chem. Soc.* **1994**, *116* (5), 1880–1889.

(65) Wade, C. R.; Broomsgrove, A. E. J.; Aldridge, S.; Gabbaï, F. P. Fluoride Ion Complexation and Sensing Using Organoboron Compounds. *Chem. Rev.* **2010**, *110* (7), 3958–3984.

(66) Scerba, M. T.; Bloom, S.; Haselton, N.; Siegler, M.; Jaffe, J.; Lectka, T. Interaction of a C-F Bond with the π-System of a C=C Bond Or "head On" with a Proximate C-H Bond. *J. Org. Chem.* **2012**, *77* (3), 1605–1609.

(67) Struble, M. D.; Scerba, M. T.; Siegler, M.; Lectka, T. Evidence for a Symmetrical Fluoronium Ion in Solution. *Science (80-.).* **2013**, *340* (6128), 57–60.

(68) Laube, T. X-Ray Crystal Structure Analysis of a Symmetrically Bridged Bishomocyclopropenyl Cation: 2,3-Dimethyl-7-Phenyl-2-Norbornen-7-Ylium hexafluoroantimonate(V). *J. Am. Chem. Soc.* **1989**, *111* (26), 9224–9232.

(69) Chai, J.-D.; Head-Gordon, M. Long-Range Corrected Hybrid Density Functionals with Damped Atom–atom Dispersion Corrections. *Phys. Chem. Chem. Phys.* **2008**, *10* (44), 6615.

(70) Grabowski, S. J. Red-and Blue-Shifted Hydrogen Bonds: The Bent Rule from Quantum Theory of

Atoms in Molecules Perspective. *J. Phys. Chem. A* **2011**, *115* (45), 12789–12799.

(71) Ferguson, L. N. Orientation of Substitution in the Benzene Nucleus. *Chem. Rev.* **1952**, *50* (1), 47–67.

(72) Galabov, B.; Nalbantova, D.; Schleyer, P. V. R.; Schaefer, H. F. Electrophilic Aromatic Substitution: New Insights into an Old Class of Reactions. *Acc. Chem. Res.* **2016**, *49* (6), 1191–1199.

(73) Gilow, H. Substituent Effects in Electrophilic Aromatic Substitution. A Laboratory in Organic Chemistry. *J. Chem. Educ.* **1977**, *54* (7), 450.

(74) Pollitt, R. J.; Saunders, B. C. 215. Meisenheimer Complexes in the M-Dinitrobenzene Series. *J. Chem. Soc.* **1964**, *0* (0), 1132–1135.

(75) Ueda, H.; Sakabe, N.; Tanaka, J.; Furusaki, A. The Structure of Meisenheimer Complex as Determined by X-Ray Crystal Analysis. *J. Chem. Soc. J. Chem. Soc.) M.R. Crampt. V. Gold, Chem. Commun. J. Am. Chem. Soc* **1968**, *41* (89), 2866–2871.

(76) Chiavarino, B.; Crestoni, M. E.; Fornarini, S.; Lanucara, F.; Lemaire, J.; Maître, P. Meisenheimer Complexes Positively Characterized as Stable Intermediates in the Gas Phase. *Angew. Chemie - Int. Ed.* **2007**, *46* (12), 1995–1998.

(77) Glukhovtsev, M. N.; Bach, R. D.; Laiter, S. Single-Step and Multistep Mechanisms of Aromatic Nucleophilic Substitution of Halobenzenes and Halonitrobenzenes with Halide Anions: Ab Initio Computational Study. *J. Org. Chem.* **1997**, *62* (12), 4036–4046.

(78) Giroldo, T.; Xavier, L. A.; Riveros, J. M. An Unusually Fast Nucleophilic Aromatic Displacement Reaction: The Gas-Phase Reaction of Fluoride Ions with Nitrobenzene. *Angew. Chemie - Int. Ed.* **2004**, *43* (27), 3588–3590.

(79) Murphy, K. E.; Bocanegra, J. L.; Liu, X.; Chau, H.-Y. Y. K.; Lee, P. C.; Li, J.; Schneebeli, S. T. Precise through-Space Control of an Abiotic Electrophilic Aromatic Substitution Reaction. *Nat. Commun.* **2017**, *8*, 14840.

(80) Meyer, E. A.; Castellano, R. K.; Diederich, F. Interactions with Aromatic Rings in Chemical and Biological Recognition. *Angewandte Chemie - International Edition*. Wiley-Blackwell March 17, 2003, pp 1210–1250.

(81) Ji, X.; Zhang, P.; Armstrong, R. N.; Gilliland, G. L. The Three-Dimensional Structure of a Glutathione S-Transferase from the Mu Gene Class. Structural Analysis of the Binary Complex of Isoenzyme 3-3 and Glutathione at 2.2-Å Resolution. *Biochemistry* **1992**, *31* (42), 10169–10184.

(82) Xiao, G.; Liu, S.; Ji, X.; Johnson, W. W.; Chen, J.; Parsons, J. F.; Stevens, W. J.; Gilliland, G. L.; Armstrong, R. N. First-Sphere and Second-Sphere Electrostatic Effects in the Active Site of a Class Mu Glutathione Transferase. *Biochemistry* **1996**, *35* (15), 4753–4765.

(83) Sulpizi, M.; Carloni, P. Cation-π versus OH-π Interactions in Proteins: A Density Functional Study. *J. Phys. Chem. B* **2000**, *104* (43), 10087–10091.

(84) Kryger, G.; Silman, I.; Sussman, J. L. Structure of Acetylcholinesterase Complexed with E2020 (Ariceptρ): Implications for the Design of New Anti-Alzheimer Drugs. *Structure* **1999**, *7* (3), 297–307.

(85) Kryger, G.; Silman, I.; Sussman, J. L. Three-Dimensional Structure of a Complex of E2020 with Acetylcholinesterase from Torpedo Californica. In *Journal of Physiology Paris*; Elsevier, 1998;

Vol. 92, pp 191–194.

(86) Banerjee, P.; Chakraborty, T. Correlation of νoH Spectral Shifts of Phenol-Benzene O-H⋯ Hydrogen-Bonded Complexes with Donor's Acidity: A Combined Matrix Isolation, Infrared Spectroscopy, and Quantum Chemistry Study. *J. Phys. Chem. A* **2014**, *118* (34), 7074–7084.

(87) Malenov, D. P.; Janjić, G. V.; Veljković, D. Ž.; Zarić, S. D. Mutual Influence of Parallel, CH/O, OH/π and Lone Pair/π Interactions in Water/benzene/water System. *Comput. Theor. Chem.* **2013**, *1018*, 59–65.

(88) Saggu, M.; Levinson, N. M.; Boxer, S. G. Direct Measurements of Electric Fields in Weak OH⋯π Hydrogen Bonds. *J. Am. Chem. Soc.* **2011**, *133* (43), 17414–17419.

(89) Mohan, N.; Vijayalakshmi, K. P.; Koga, N.; Suresh, C. H. Comparison of Aromatic NH⋯π, OH⋯π, and CH⋯π, Interactions of Alanine Using MP2, CCSD, and DFT Methods. *J. Comput. Chem.* **2010**, *31* (16), 2874–2882.

(90) Tóth, G.; Bowers, S. G.; Truong, A. P.; Probst, G. The Role and Significance of Unconventional Hydrogen Bonds in Small Molecule Recognition by Biological Receptors of Pharmaceutical Relevance. *Curr. Pharm. Des.* **2007**, *13* (34), 3476–3493.

(91) Motherwell, W. B.; Moïse, J.; Aliev, A. E.; Nič, M.; Coles, S. J.; Horton, P. N.; Hursthouse, M. B.; Chessari, G.; Hunter, C. A.; Vinter, J. G. Non-covalent Functional-Group-Arene Interactions. *Angew. Chemie - Int. Ed.* **2007**, *46* (41), 7823–7826.

(92) Aliev, A. E.; Arendorf, J. R. T.; Pavlakos, I.; Moreno, R. B.; Porter, M. J.; Rzepa, H. S.; Motherwell, W. B. Surfing ?? Clouds for Non-covalent Interactions: Arenes versus Alkenes. *Angew. Chemie - Int. Ed.* **2015**, *54* (2), 551–555.

(93) Ferguson, G.; Gallagher, J. F.; Glidewell, C.; Zakaria, C. M. O–H.π(arene) Intermolecular Hydrogen Bonding in the Structure of 1,1,2-Triphenylethanol. *Acta Crystallogr. Sect. C Cryst. Struct. Commun.* **1994**, *50* (1), 70–73.

(94) Paruch, K.; Vyklický, L.; Wang, D. Z.; Katz, T. J.; Incarvito, C.; Zakharov, L.; Rheingold, A. L. Functionalizations of [6]- and [7]Helicenes at Their Most Sterically Hindered Positions. *J. Org. Chem.* **2003**, *68* (22), 8539–8544.

(95) Hong, J.; Yang, G.-S.; Duan, C.-Y.; Guo, Z.-J.; Zhu, L.-G. Fluorescence Quenching of EB – DNA Complex by a Novel Di-Bipyridyl Ruthenium (II) Complex of P - Tert -Butyltetrathiacalix [4] Arene. *Inorg. Chem. Commun.* **2005**, *8* (11), 988–991.

(96) Carr, G. E.; Chambers, R. D.; Holmes, T. F.; Parker, D. G. Sodium Perfluoroalkane Carboxylates as Sources of Perfluoroalkyl Groups. *J. Chem. Soc. Perkin Trans. 1* **1988**, *0* (4), 921.

(97) Gustafson, J. L.; Lim, D.; Miller, S. J. Dynamic Kinetic Resolution of Biaryl Atropisomers via Peptide-Catalyzed Asymmetric Bromination. *Science (80-.).* **2010**, *328* (5983), 1251–1255.

(98) Pathak, T. P.; Miller, S. J. Site-Selective Bromination of Vancomycin. *J. Am. Chem. Soc.* **2012**, *134* (14), 6120–6123.

(99) Rosenthal, J.; Schuster, D. I. The Anomalous Reactivity of Fluorobenzene in Electrophilic Aromatic Substitution and Related Phenomena. *J. Chem. Educ.* **2003**, *80* (6), 679.

(100) Roberts, J. D.; Sanford, J. K.; Sixma, F. L. J.; Cerfontain, H.; Zagt, R. Orientation in Aromatic Nitration Reactions. *J. Am. Chem. Soc.* **1954**, *76* (18), 4525–4534.

(101) Nieves-Quinones, Y.; Singleton, D. A. Dynamics and the Regiochemistry of Nitration of Toluene.

J. Am. Chem. Soc. **2016**, *138* (46), 15167–15176.

(102) Reich, H. J.; Cram, D. J. Macro Rings. XXXV. Transannular Directive Influences in Electrophilic Substitution of Monosubstituted [2.2]Paracyclophanes. *J. Am. Chem. Soc.* **1969**, *91* (13), 3505–3516.

(103) Bondarenko, L.; Kampf, J. W.; Lahann, J. The Synthesis of Brominated tetrafluoro[2.2]paracyclophanes. *European J. Org. Chem.* **2006**, *2006* (24), 5499–5504.

(104) Carey, F. A. ORGANIC CHEMISTRY.

(105) Diels, O.; Alder, K. Synthesen in Der Hydroaromatischen Reihe. X. Mitteilung: ???Dien???Synthesen??? Mit Pyrrol Und Seinen Homologen. *Justus Liebigs Ann. Chem.* **1931**, *486* (1), 211–225.

(106) McMurry, J. E.; Lectka, T. Three-Center, Two-Electron C-H-C Bonds in Organic Chemistry. *Acc. Chem. Res.* **1992**, *25* (1), 47.

(107) Bader, R. F. W. Atoms in Molecules. *Acc. Chem. Res.* **1985**, *18* (1), 9–15.

(108) Tuncel, D.; Özsar, Ö.; Tiftik, H. B.; Salih, B. Molecular Switch Based on a cucurbit[6]uril Containing Bistable [3]rotaxane. *Chem. Commun.* **2007**, *0* (13), 1369–1371.

(109) Huang, Y.-L.; Hung, W.-C.; Lai, C.-C.; Liu, Y.-H.; Peng, S.-M.; Chiu, S.-H. Using Acetate Anions To Induce Translational Isomerization in a Neutral Urea-Based Molecular Switch. *Angew. Chemie Int. Ed.* **2007**, *46* (35), 6629–6633.

(110) Struble, M. D.; Holl, M. G.; Coombs, G.; Siegler, M. A.; Lectka, T. Synthesis of a Tight Intramolecular OH···Olefin Interaction, Probed by IR, 1H NMR, and Quantum Chemistry. *J. Org. Chem.* **2015**, *80* (9), 4803–4807.

(111) Guan, L.; Holl, M. G.; Pitts, C. R.; Struble, M. D.; Siegler, M. A.; Lectka, T. Through-Space Activation Can Override Substituent Effects in Electrophilic Aromatic Substitution. *J. Am. Chem. Soc.* **2017**, *139* (42), 14913–14916.

Curriculum Vitae

Liangyu Guan Email: liangyuguan50@gmail.com

EDUCATION:

Aug. 2014 – May. 2018 The Johns Hopkins University
Ph.D. of Chemistry (with professor Thomas Lectka)

Sep. 2012 – Aug. 2014 Western Michigan University
M.S of Chemistry (with professor Yirong Mo)

Sep. 2007 – Jun. 2011 Tianjin University of Science and Technology
B.S of Chemistry

AWARDS AND HONORS:

Apr. 2014 Outstanding Graduate Research Award.

Nov. 2009 First Class Prize in Contemporary Undergraduate Mathematical Contest in Modeling (China).

2008-2010 Scholarship for Academic Excellence (3 times).

WORK EXPERIENCES:

Aug.2014 – May. 2018 Teaching assistant and research assistant in chemistry department (JHU)

Sep. 2013 – Aug. 2014 Research assistant in associate professor Yirong Mo's Lab.

Aug. 2012 – Jun. 2013 Teaching assistant in chemistry department (WMU).

RESEARCH EXPERIENCES:

Jan. 2015 – May. 2018

Institution: The Johns Hopkins University

Project: The effect of through-space interaction on molecular reactivity.

Mar. 2013 – Aug. 2014

Institution: Western Michigan University

Project: Computational chemistry; the Nature of Pnicogen Bond: Block-localized Wavefunction (BLW) Energy Decomposition Method

Mar.2010 – Jun. 2011

Institution: College of Science, Tianjin University of Science and Technology

Project: Studies on Synthesis and Modification of Anti-HIV Active Nucleoside 5'-Thiophosphoramidates Derivatives

Jun.2010 – Sep. 2010

Institution: Department of Material Science and Technology, Beijing University of Chemical Technology

Laboratory: Key Lab of Material Environmental Behavior and Surface Protection

Project: Studies on Corrosion and Inhibition Behavior of Carbon Steel

PUBLICATION:

(1) **Guan, L**.; Holl, M. G.; Pitts, C. R.; Struble, M. D.; Siegler, M. A.; Lectka, T. Through-Space Activation Can Override Substituent Effects in Electrophilic Aromatic Substitution. J. Am. Chem. Soc. 2017.

(2) Struble, M. D.; **Guan, L**.; Siegler, M. A.; Lectka, T. A C–F Bond Directed Diels–Alder Reaction. J. Org. Chem. 2016, 81 (17), 8087–8090.

(3) Mo, Y.; Ahmed, B. M.; **Guan, L**.; Karty, J.; Mezei, G. Deprotonation of Methyl-Substituted, Five-Membered Aromatic Molecules: A Surprising Case of Mixed Conjugation, Rehybridization, and Induction Contributions. Org. Lett. 2014, 16 (17), 4680–4683.

(4) Wang, C.; **Guan, L**.; Danovich, D.; Shaik, S.; Mo, Y. The Origins of the Directionality of Noncovalent Intermolecular Interactions. Journal of Computational Chemistry. 2015, 37 (1), 34-45.

(5) Mo, Y.; Wang, C.; **Guan, L**.; Braida, B.; Hiberty, P. C.; Wu, W. On the Nature of Blueshifting Hydrogen Bonds. Chemistry-A European Journal 2014 20 (27), 8444-8452.

(6) **Guan, L**.; Mo, Y. Electron Transfer in Pnicogen Bonds. J. Phys. Chem. A 2014, 118 (39), 8911–8921.

RESEARCH INTERESTS:

Organic Synthesis

Computational Chemistry

Material Science and Engineering